SM and Higgs physics results

Ezio Torassa

Università di Padova e Sezione dell'INFN, Padova.

On behalf of CMS and ATLAS

SSI2016: 44th SLAC Summer Institute – New Horizons on the Energy Frontier
August 15-26 2016, SLAC, Menlo Park, California

Overview

① Introduction

② SM: cross section measurements

③ SM: anomalous gauge couplings

④ SM: top mass

⑤ SM: angular analysis of $B^0 \rightarrow K^{*}\mu\mu$

⑥ Higgs introduction and electroweak fits

⑦ Higgs mass

⑧ Higgs cross section

⑨ Higgs signal strength and coupling modifiers

⑩ Higgs decay width

11 Higgs spin and parity

12 Outlook

13 Summary

① Introduction: ALTAS vs CMS

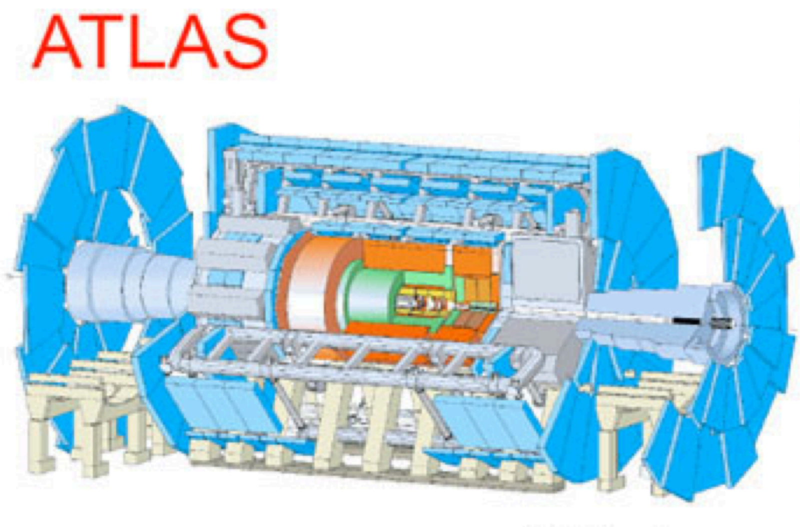

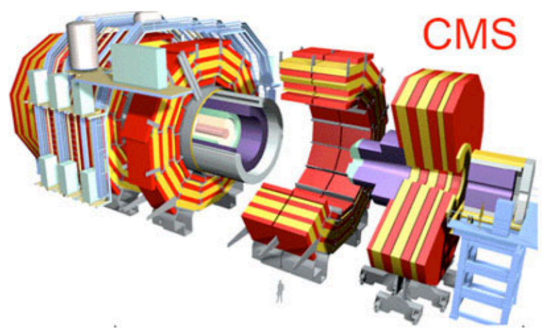

	ATLAS	CMS
Diameter (m)	25	15
Lenght (m)	46	21
Weight (tons)	7000	12,500
Solenoid magnetic field (T)	2	4

	ATLAS	CMS
Tracking p_T resoluiton		Higher magnefic field
Standalone muon tracking	Less multiple scattering	
Jet and E_{miss} resolution	Higher λ for HCAL	
e/γ energy resolution		Higher ECAL resolution

① Introduction: luminosity

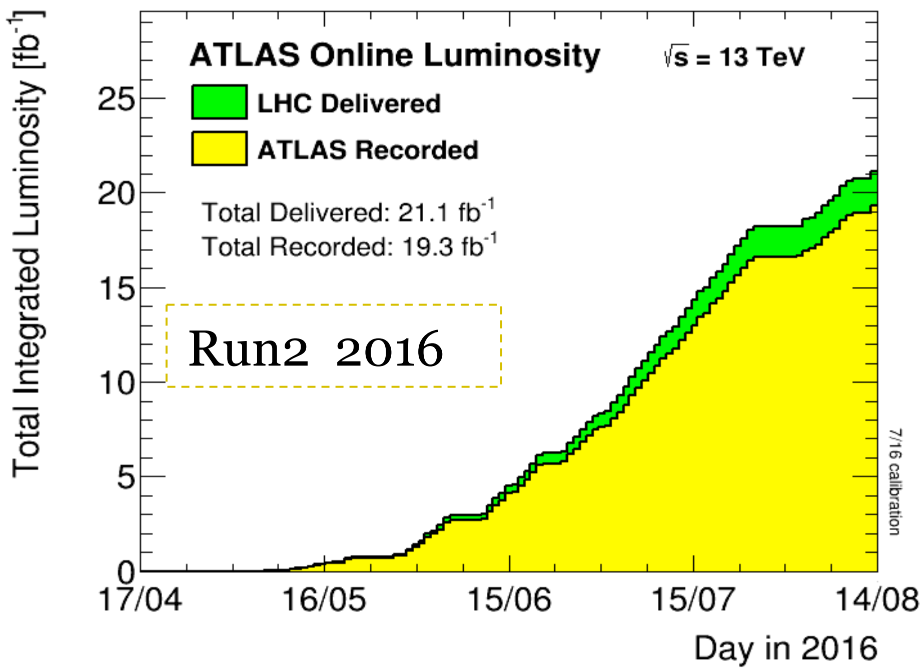

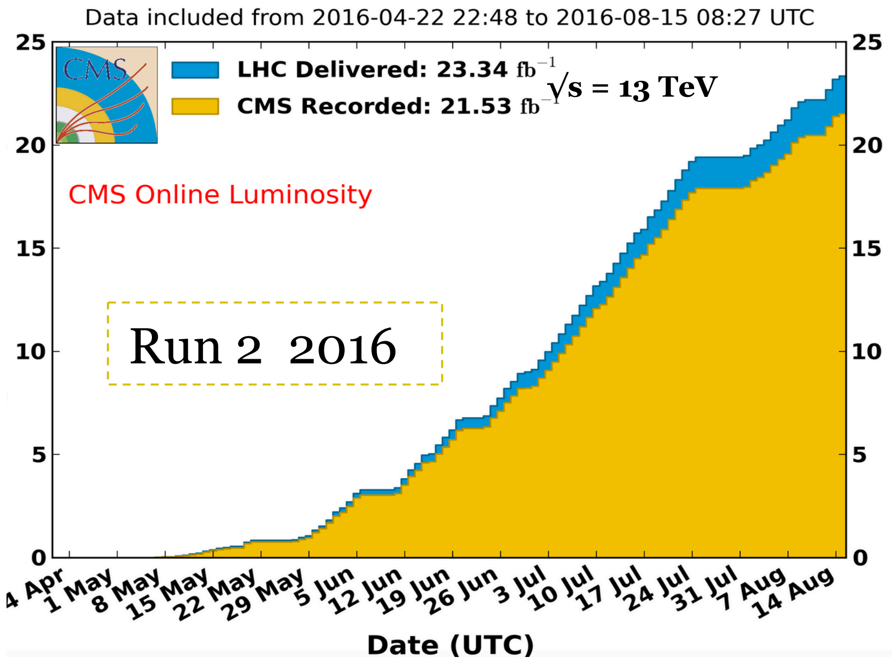

Run 1	2011: 7 TeV	2012: 8 TeV
LHC delivered to ATLAS / CMS	5.5 fb^{-1} / 6.1 fb^{-1}	22.8 fb^{-1} / 23.3 fb^{-1}
Recorded by ATLAS / CMS	5.1 fb^{-1} / 5.5 fb^{-1}	21.3 fb^{-1} / 21.8 fb^{-1}

Run 2	2015: 13 TeV	2016: 13 TeV
LHC delivered to ATLAS / CMS	4.2 fb^{-1} / 4.2 fb^{-1}	21.1 fb^{-1} / 23.3 fb^{-1}
Recorded by ATALS / CMS	3.9 fb^{-1} / 3.8 fb^{-1}	19.3 fb^{-1} / 21.5 fb^{-1}

② SM: cross section measurements

- Precise cross section measurements can provide better estimation of the Higgs backgrounds (e.g. , WW is the main background of the H-> WW channel)

- Also with no evidence of light new resonances ($M_{\text{new physics}} >> E^{\text{LHC}}$) the new physics can affect the differential cross section in the high mass region. The deviation from the SM expectation can be expressed with an effective field theory

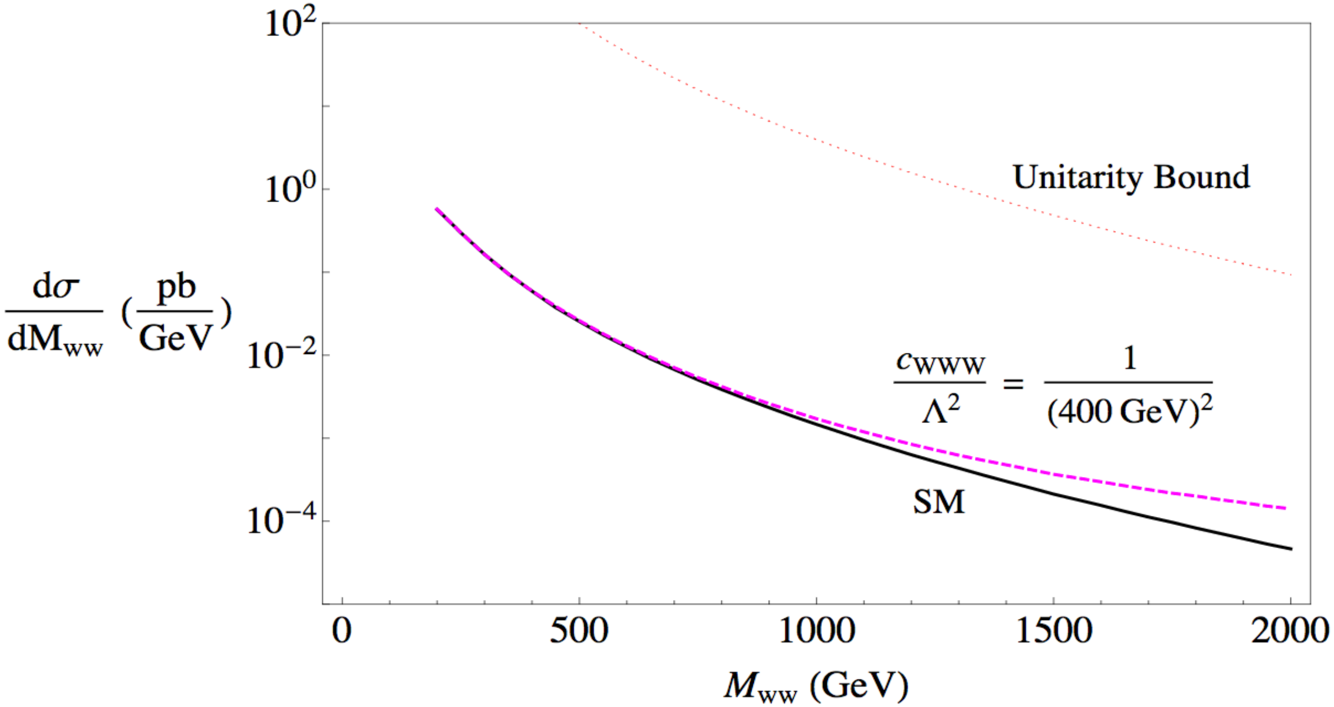

arXiv:1205.4231

② SM: CMS cross section measurements

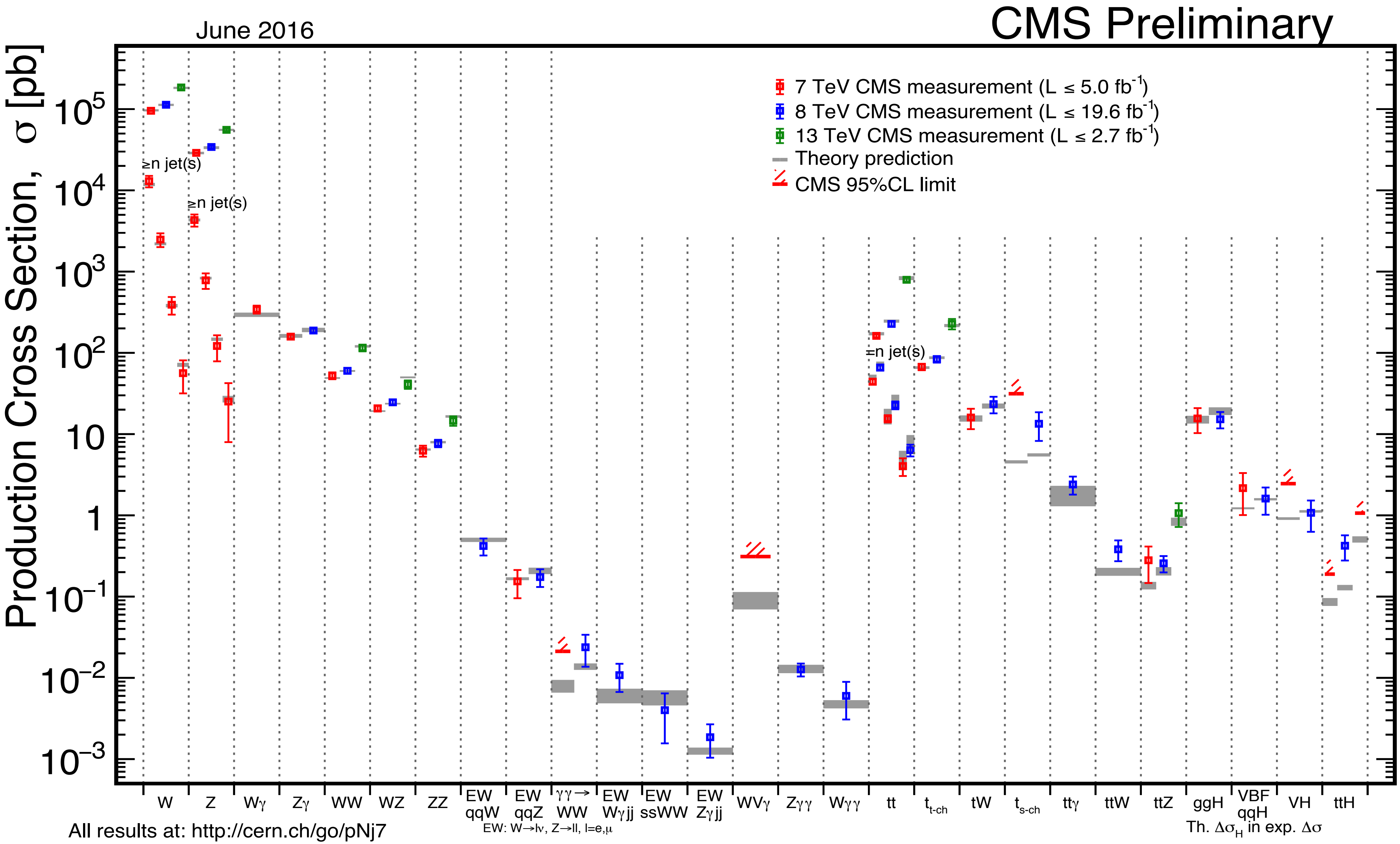

② SM: ATLAS cross section measurements

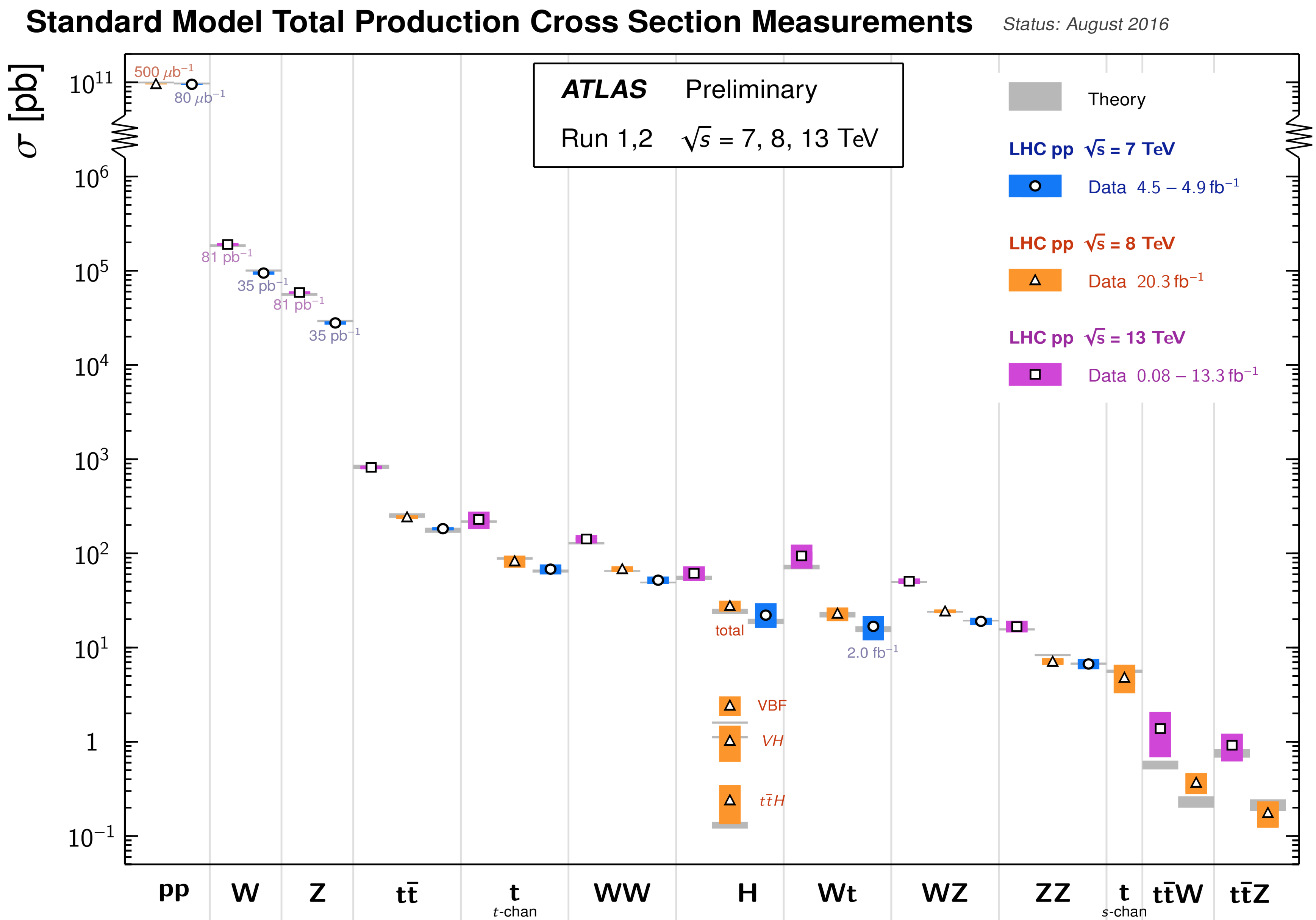

② SM: CMS cross section measurements

1) CMS-PAS-SMP-16-006 WW cross section 13 TeV 2.3 fb^{-1} June 2016
2) CMS-PAS-SMP-16-002 WZ cross section 13 TeV 2.3 fb^{-1} July 2016
3) CMS-PAS-SMP-16-001 ZZ cross section 13 TeV 2.3 fb^{-1} July 2016

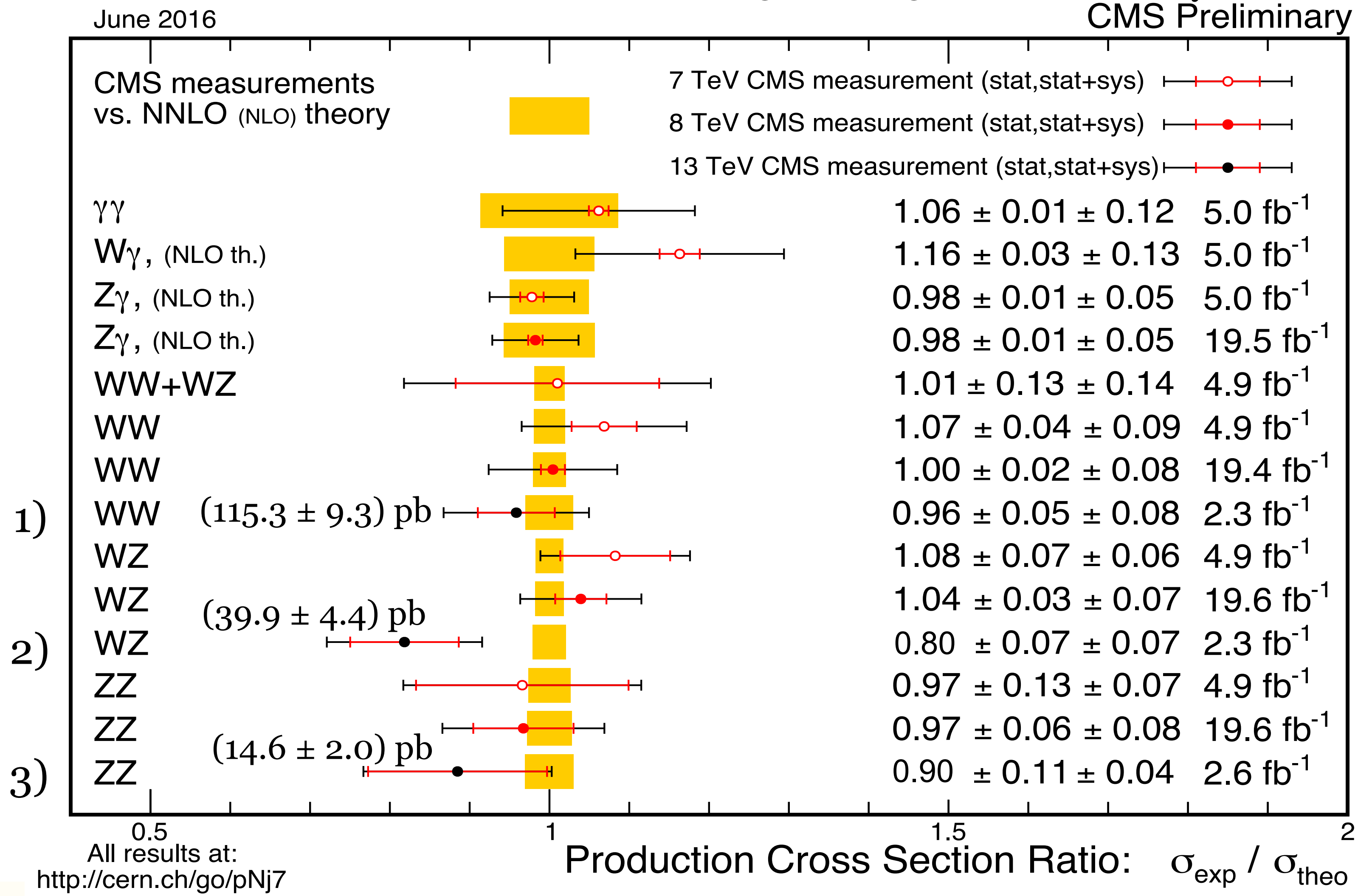

② SM: ATLAS cross section measurements

1)	ATLAS-CONF-2016-090	WW cross section	13 TeV	3.2 fb^{-1}	4th August 2016
2)	arXiv:1606.04017	WZ cross section	13 TeV	3.2 fb^{-1}	June 2016
3)	Phys. Rev. Lett. 116, 101801 (2016)	ZZ cross section	13 TeV	3.2 fb^{-1}	December 2015

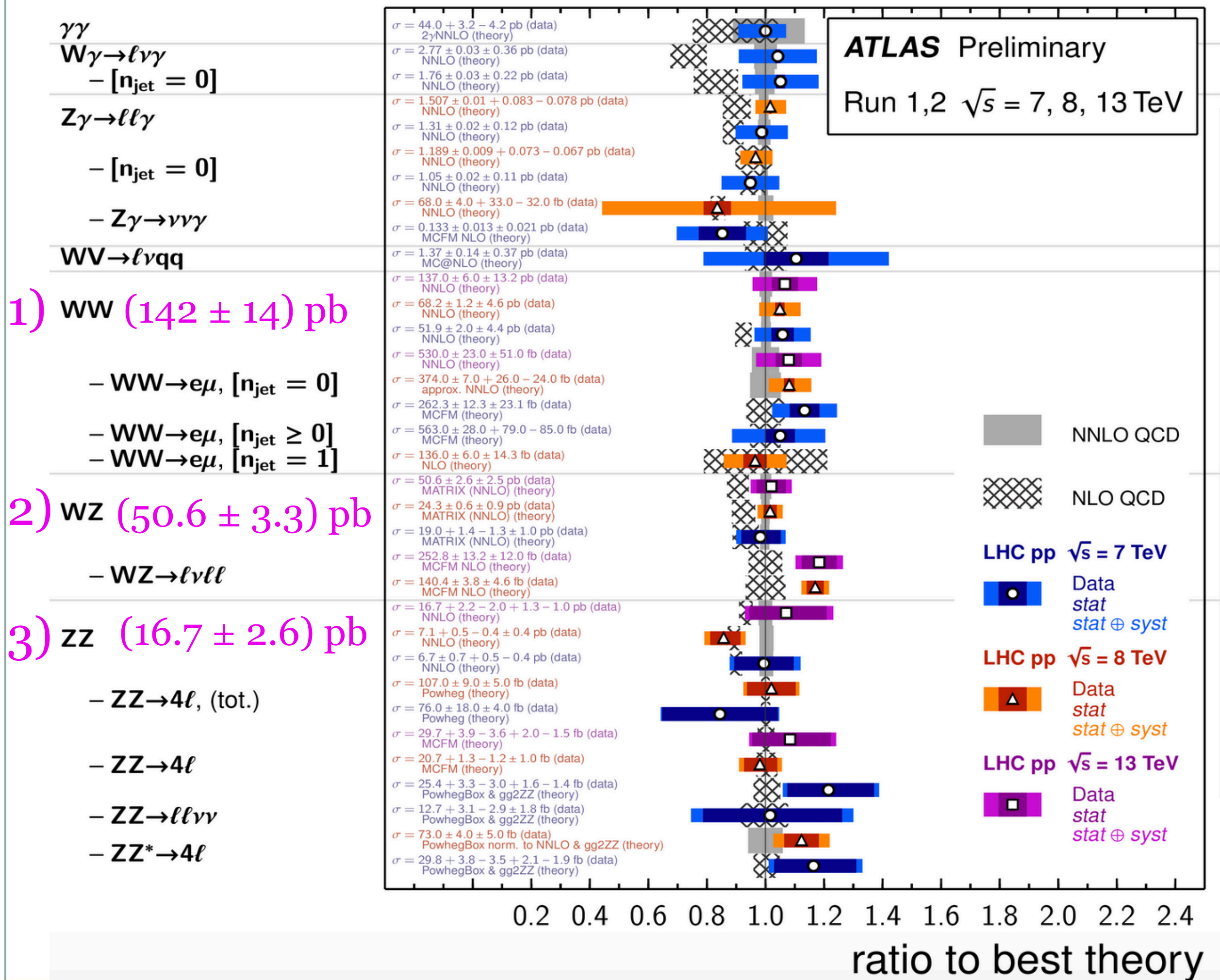

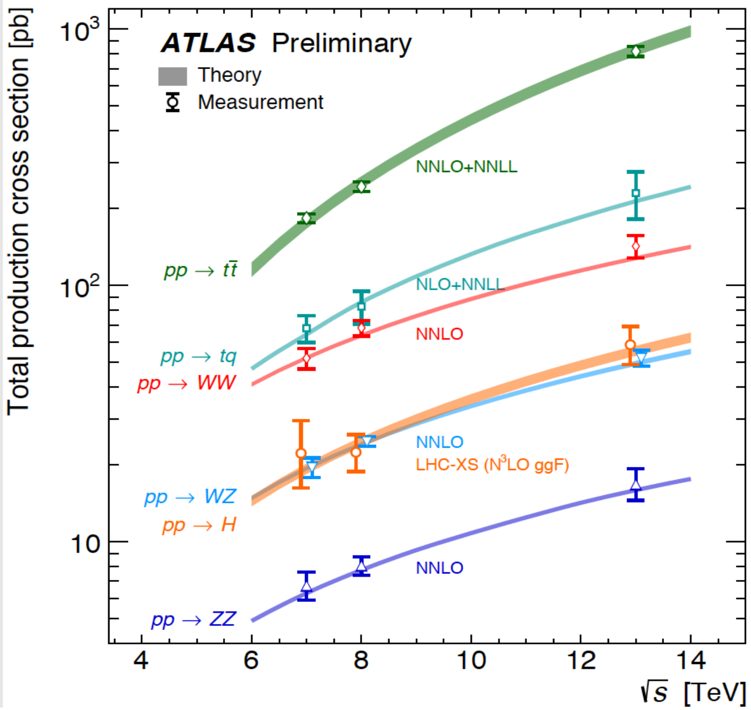

② SM: inelastic cross section

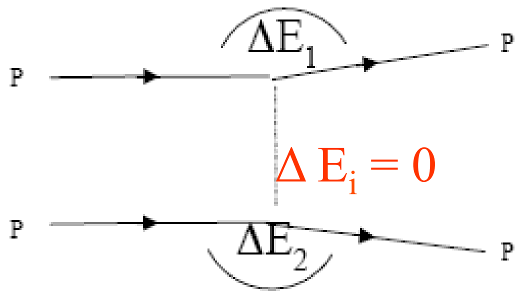

Elastic scattering (25%)

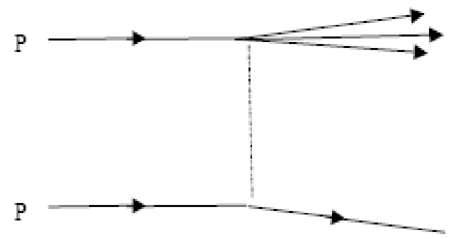

Single diffractive inelastic (8%)

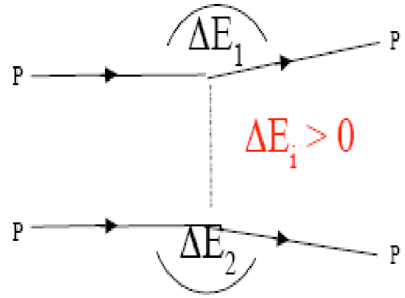

Double diffractive inelastic (8%)

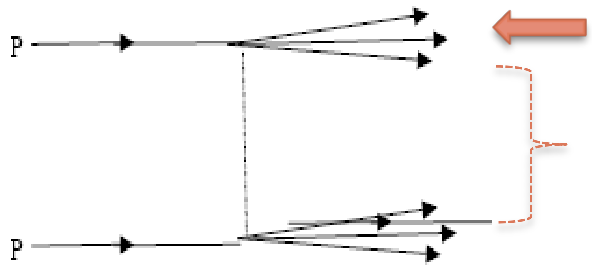

M_X= invariant mass of the collection of tracks

Collections are separated with the largest rapidity gap

Not diffractive inelastic (55%)

The cross section measurement excludes elastic pp scattering and diffractive dissociation processes with M_X<13 GeV, or equivalently, $\xi = M^2_X/s < 10^{-6}$

In the fiducial region $\xi > 10^{-6}$ (M_X>13 GeV) the event selection efficiency exceeds 50%.

The total inelastic cross section is extrapolated using models of inelastic interactions.

② SM: inelastic cross section

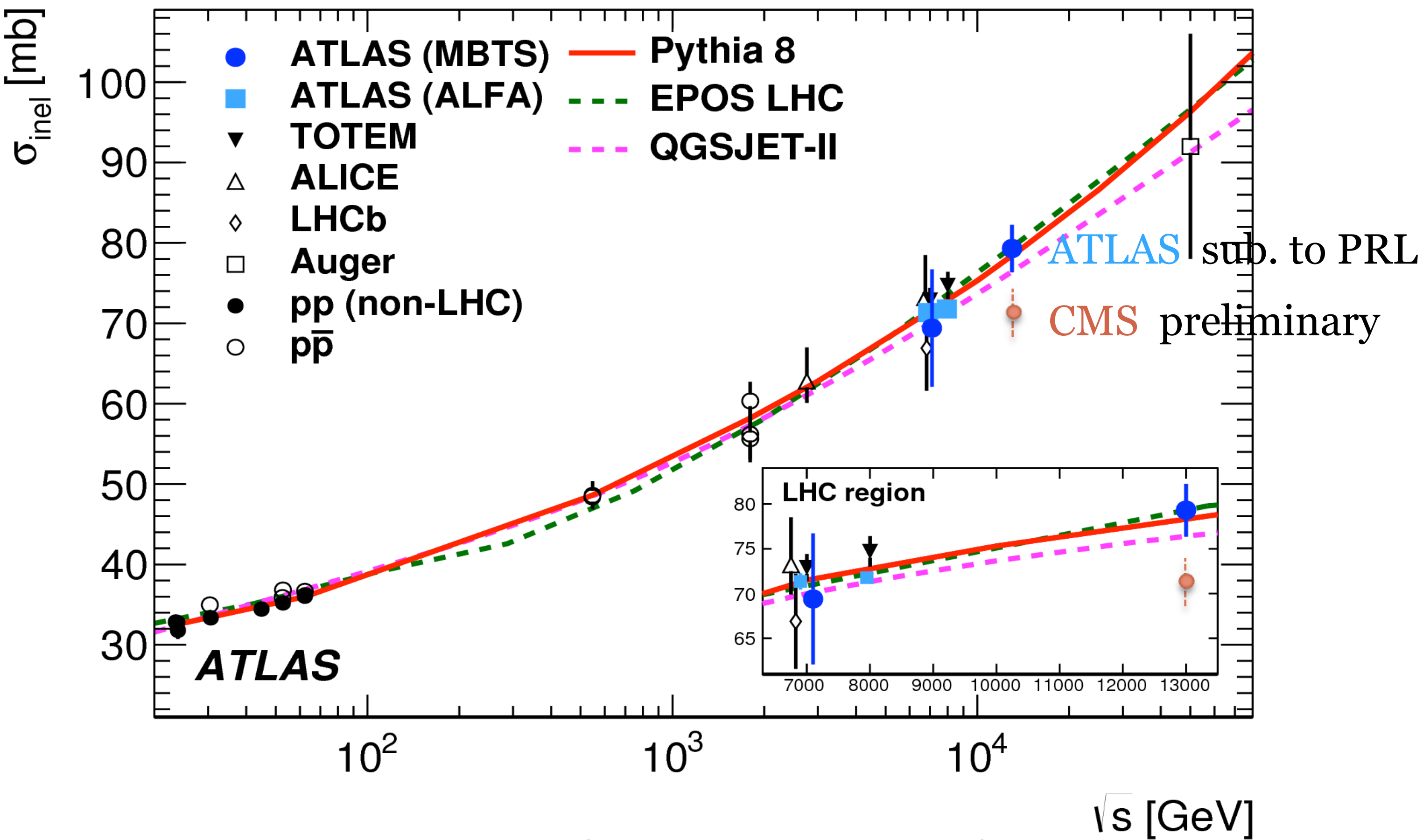

ATLAS σ_{inel}=79.3 ± 0.8 (exp) ± 1.3 (lumi) ± 2.5 (ext) mb arXiv:1606.02625

CMS σ_{inel}=71.3 ± 0.5 (exp) ± 2.1 (lumi) ± 2.7 (ext) mb CMS-PAS-FSQ-15-005

ATLAS σ^{fid}_{inel}=68.2 ± 0.8 (exp) ± 1.3 (lumi) $\xi > 10^{-6}$ $M_X > 13$ GeV

CMS σ^{fid}_{inel}=65.8 ± 0.8 (exp) ± 1.8 (lumi) $\xi > 10^{-6}$ $M_X > 13$ GeV

CMS σ^{fid}_{inel}=66.9 ± 0.4 (exp) ± 2.0 (lumi) $\xi > 10^{-7}$ $M_X > 4.1$ GeV

③ SM: limits on anomalous gauge couplings

Anomalous values of the triple and quartic gauge couplings due to the presence of new physics would change the rate of the di-bosons and tri-bosons final states.
Limits on anomalous (e.g. , WWZ) couplings can be expressed in term of the possible deviation from zero of the parameters:

$$\Delta k_Z = k_Z - 1 \qquad \lambda_z = \lambda_\gamma \qquad \Delta g_1^Z = g_1^Z - 1$$

(introduced to express the most general Lorentz invariant W W Z vertex)

Limits on WWZ triple gluon couplings

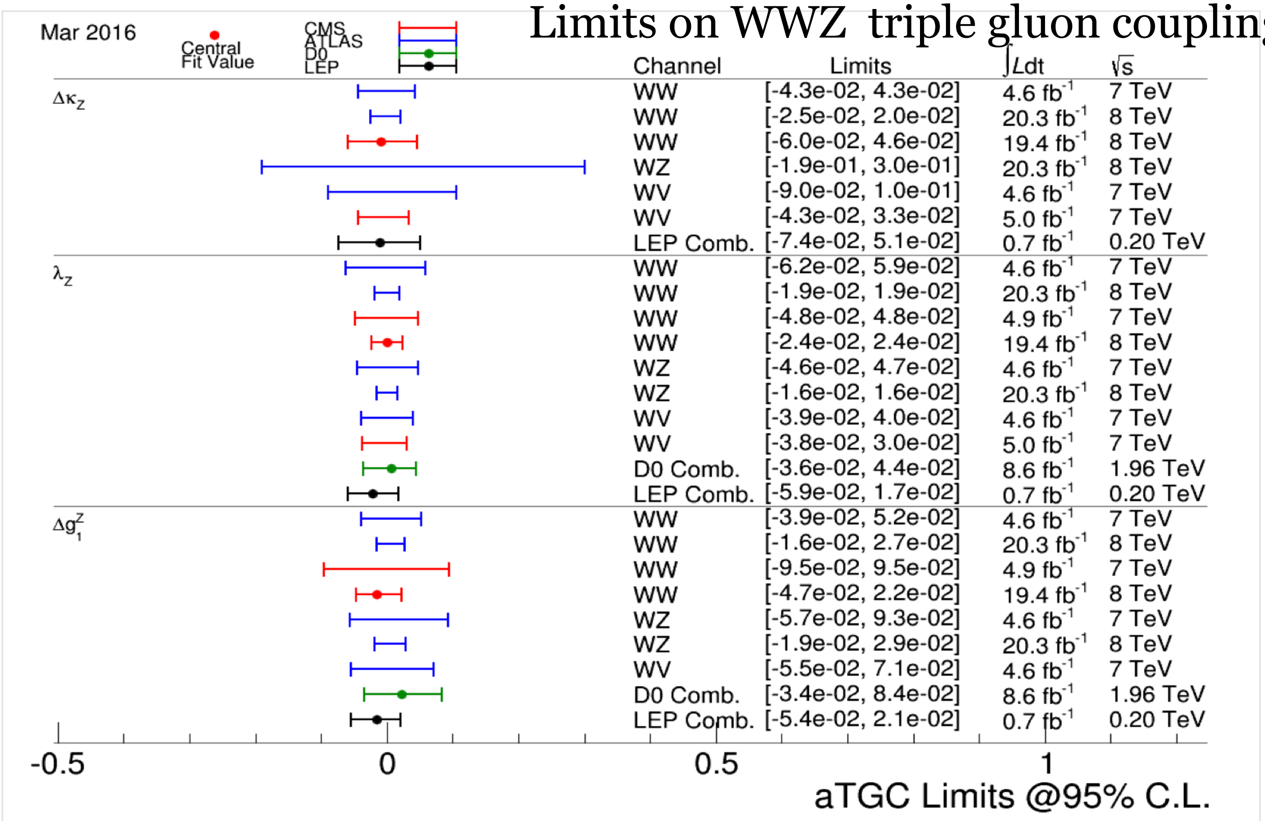

④ SM: top mass

Precise m_{top} measurements provide critical inputs to the global electroweak fits that help to test the internal consistency of the SM

Word combination (March 2014)

m_{top} = 173.34 ± 0.36 (stat) ± 0.67 (syst) GeV
= 173.34 ± 0.76 GeV

Tevatron (arXiv:1407.2682, July 2014, 9.7 fb^{-1})
(proton-antiproton collisions at 1.96 TeV)

m_{top} = 174.34 ± 0.37 (stat) ± 0.52 (syst) GeV
= 174.34 ± 0.64 GeV

CMS RUN1 (Phys. Rev. D 93, 072004, 7 April 2016)

m_{top} = 172.44 ± 0.13 (stat) ± 0.47 (syst) GeV
= 172.44 ± 0.48 GeV

hadr.~0.35 GeV
JES~0.15 GeV

ATLAS RUN1 (arXiv:1606.02179, 7 June 2016)

m_{top} = 172.84 ± 0.34 (stat) ± 0.61 (syst) GeV
= 172.84 ± 0.70 GeV

hadr.~0.23 GeV
JES~0.41 GeV

LHC top WG Aug 2016

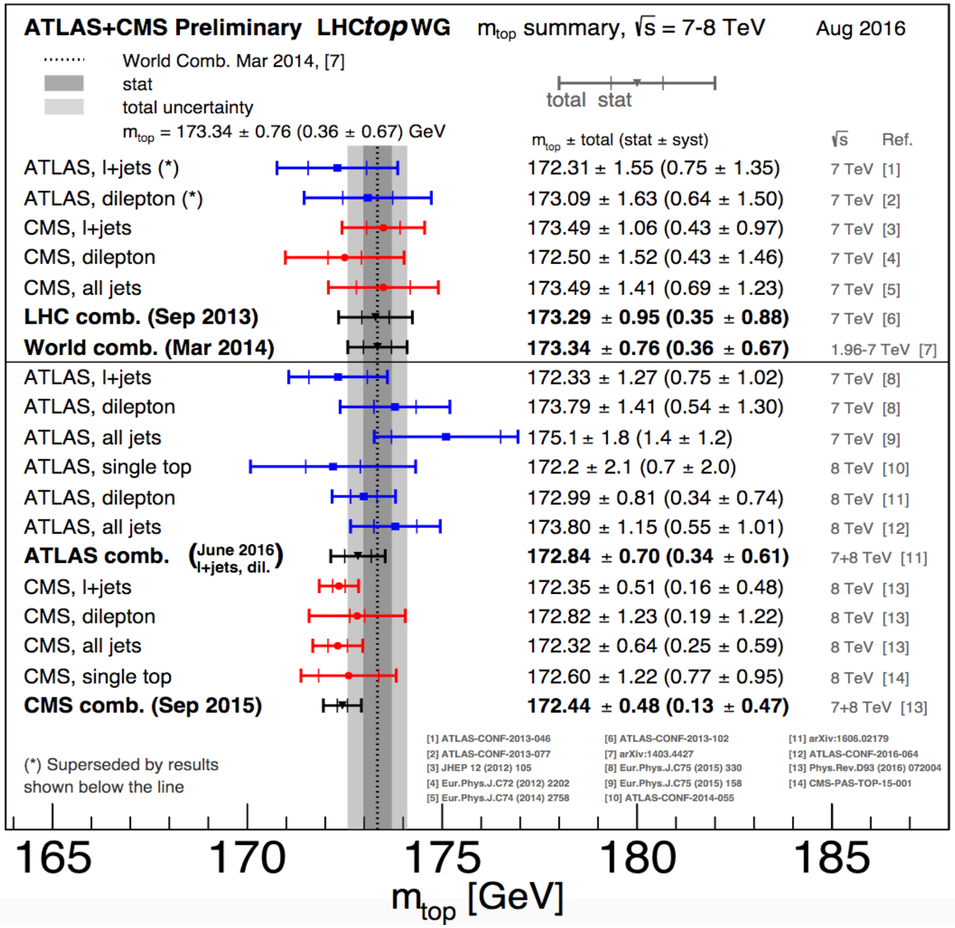

⑤ SM: angular analysis of $B^o \to K^*\mu\mu$

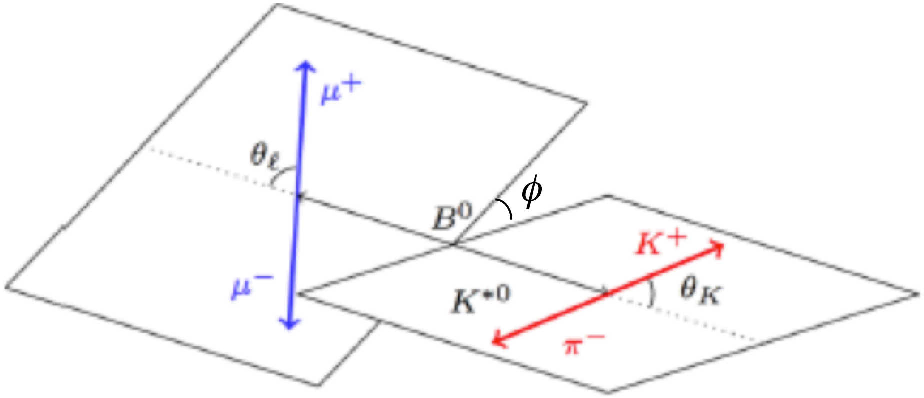

Differential Amplitude:

$$\frac{1}{\Gamma}\frac{d^3\Gamma}{d\vec{\Omega}} = \frac{1}{\Gamma}\frac{d^3\Gamma}{d\vec{\Omega}}\bigg|_P + \frac{3}{16\pi}F_S \sin^2\theta_l\bigg|_S + \text{S-P interf.}$$

P wave K^* S wave pollution ~10%

$$\frac{1}{\Gamma}\frac{d^3\Gamma}{d\vec{\Omega}}\bigg|_P = \frac{9}{32\,\pi}\Big[\frac{3}{4}(1-F_L)\sin^2\theta_K + F_L\cos^2\theta_K + \frac{1}{4}(1-F_L)\sin^2\theta_K\cos 2\theta_l - F_L\cos^2\theta_K\cos 2\theta_l$$

$$+ S_3\sin^2\theta_K\sin^2\theta_l\cos 2\phi + S_4\sin 2\theta_K\sin 2\theta_l\cos\phi + S_5\sin 2\theta_K\sin\theta_l\cos\phi$$

$$+ \frac{4}{3}A_{FB}\sin^2\theta_K\cos\theta_l$$

$$+ S_7\sin 2\theta_K\sin\theta_l\sin\phi + S_8\sin 2\theta_K\sin 2\theta_l\sin\phi + S_9\sin^2\theta_K\sin^2\theta_l\sin 2\phi\Big]$$

F_L : fraction of longitudinally polarized K*

A_{FB}: forward-backward muon asimmetry

(independent from ϕ)

⑤ SM: Angular analysis of $B^o \rightarrow K^*\mu\mu$

Phys. Lett. B753, 424 (2016)

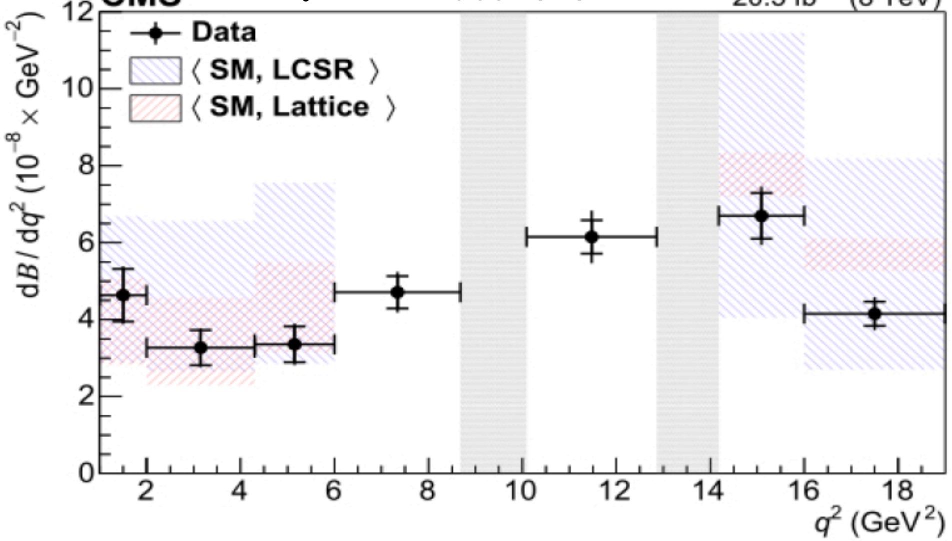

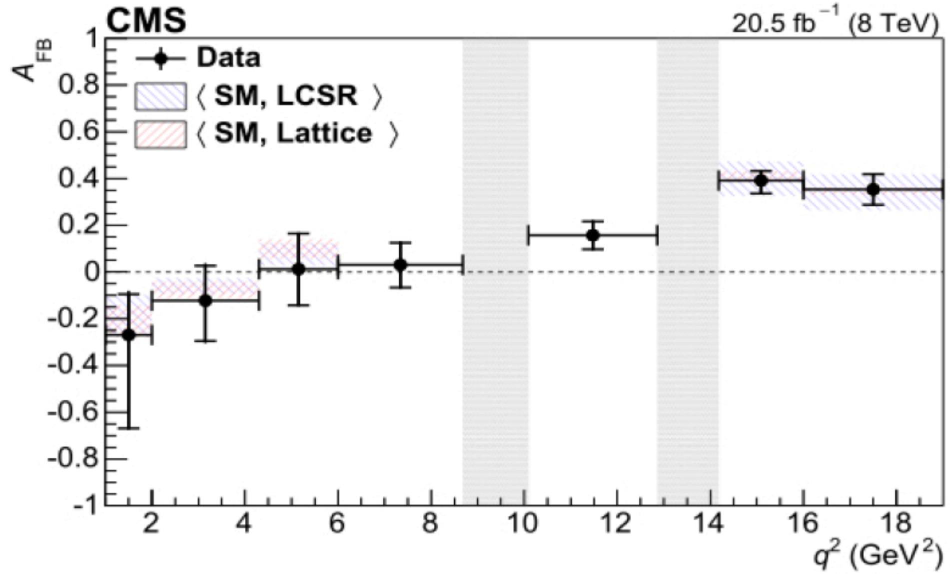

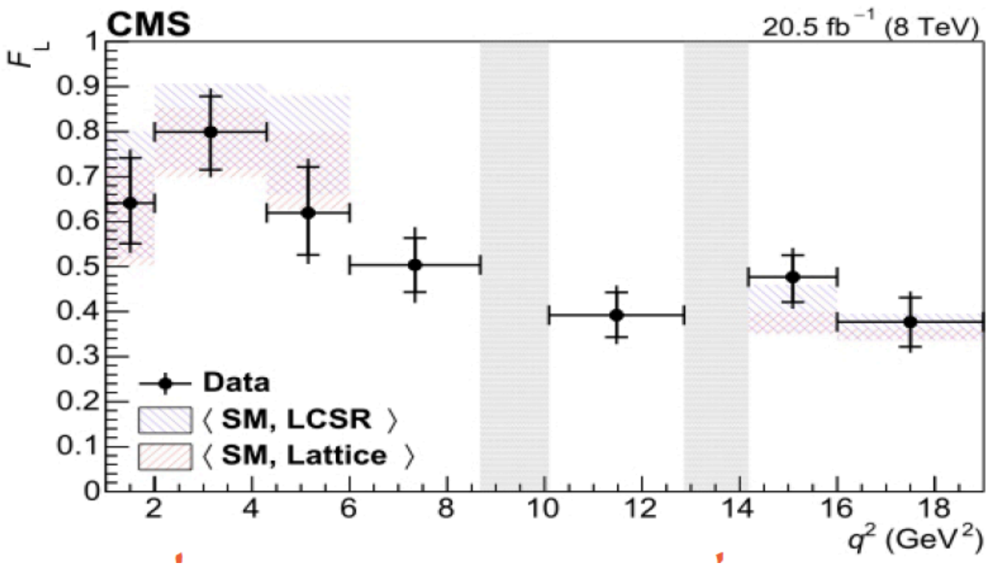

Differential amplitude consistent with SM

Expected soon: result using variable P5'
and $B+ \rightarrow K^+\mu\mu$, $K^{*+}\mu\mu$ angular analyses

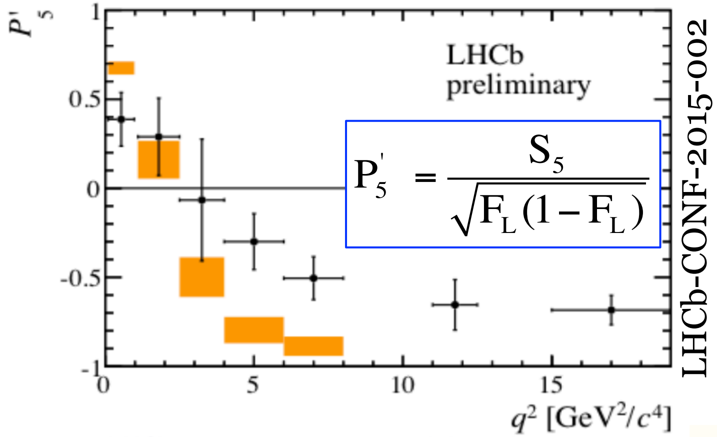

$$P_5' = \frac{S_5}{\sqrt{F_L(1-F_L)}}$$

⑥ Higgs introduction: production modes

gluongluonFusion

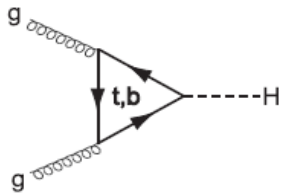

Vector Boson Fusion

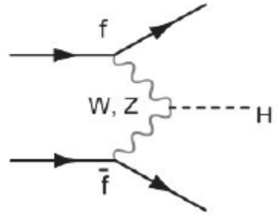

VH (Higgs-strahlung)

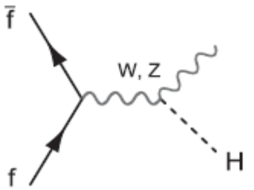

ttH

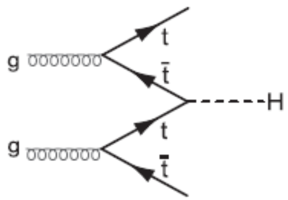

Cross section[pb] of SM 125 GeV Higgs at NNLO+NNLL QCD and NLO EW

mode	7 TeV	8 TeV	13 TeV	σ(13)/σ(8)
ggH	15	19	44	2.3
VBF	1.2	1.6	3.7	2.3
WH	0.58	0.70	1.4	2.0
ZH	0.33	0.41	0.87	2.1
ttH	0.086	0.13	0.51	3.9
bbH	0.16	0.20	0.51	2.5

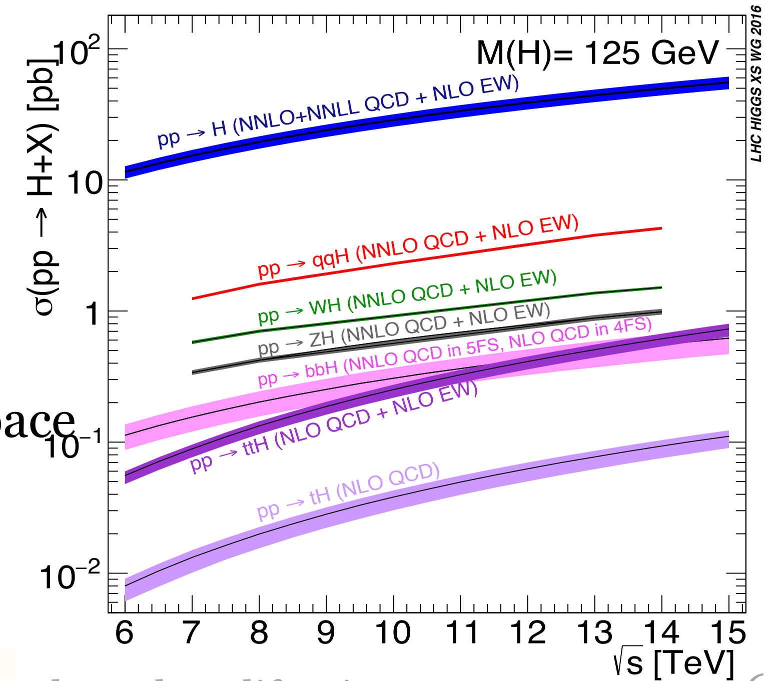

- 1 million H bosons produced during LHC Run1
  2 millions H bosons produced during LHC Run2
- all rates of production modes increase at 13 TeV
- the high rate increase of **ttH** is due to the phase space opening and the high mass system ($2m_t+m_H$)

⑥ Higgs introduction: decay channels

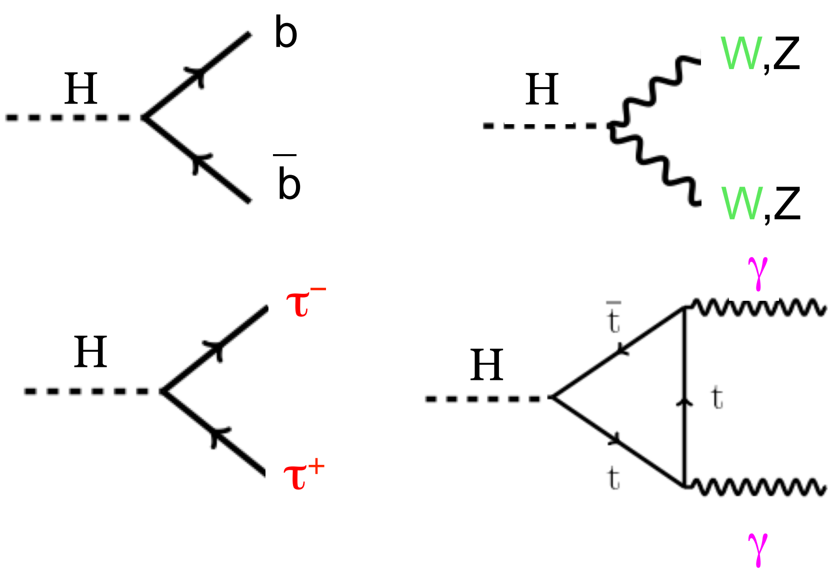

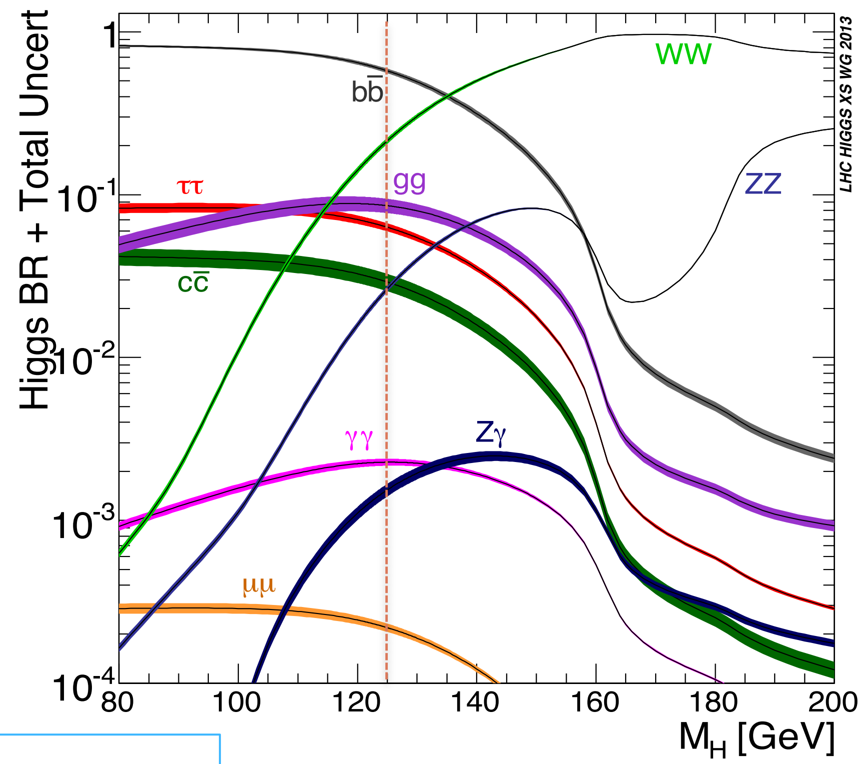

Main 6 decay channels:

H->bb	WW*	ZZ*	ττ	γγ	μμ
57.5%	21.6%	2.67%	6.30%	0.23%	0.022%

The Higgs does not couple with gluons and photons because they are massless particles anyway the **gg fusion** is the dominant contribution in the production and the H → γγ is a fundamental decay channel for the discovery and mass measurement (loops with fermions are relevant)

⑥ Electroweak fits

Precision measurements first from LEP/SLC, then Tevatron and now LHC

Physics Letters B 565 (2003) 61–75

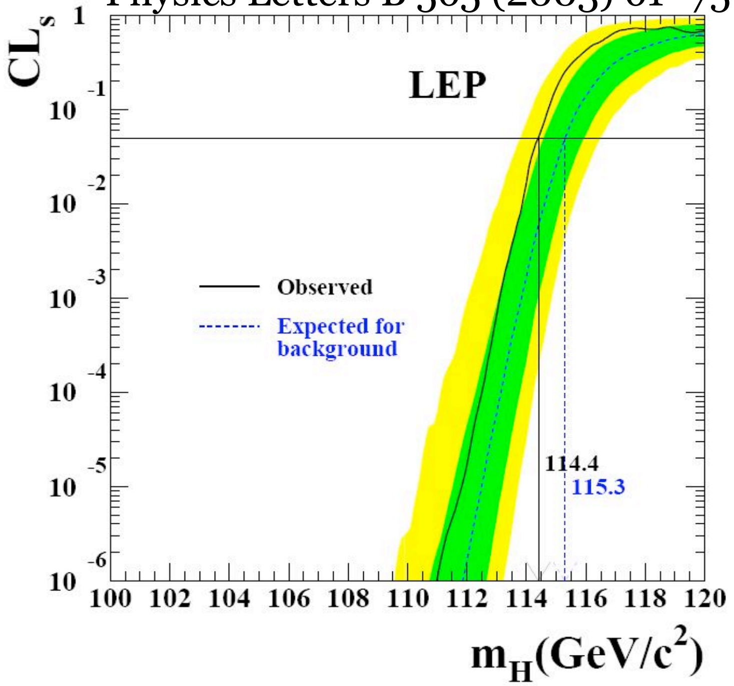

$M_H > 114.4$ GeV/c^2 at 95% CL$_s$

Eur. Phys. J. C 72, 2003 (2012)

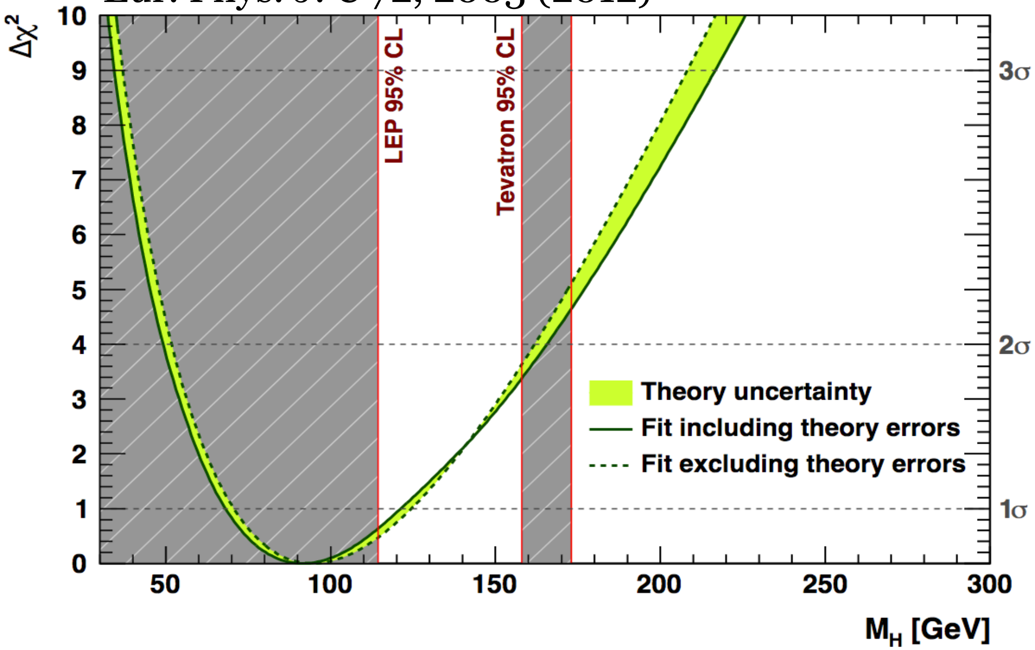

Indirect determination from EW fit (2012):

$$M_H = 96^{+31}_{-24} \text{ GeV}$$

(Direct exclusion limits also incorporated)

Fits to SM precision measurements prefer a low Higgs mass value and exclusion regions are compatible with the fit

⑦ Higgs mass: H→γγ and H→ZZ→4l

The mass is measured wit the H→γγ and H→ZZ→4l decay channels

EPCJ 74 (2014) 3076

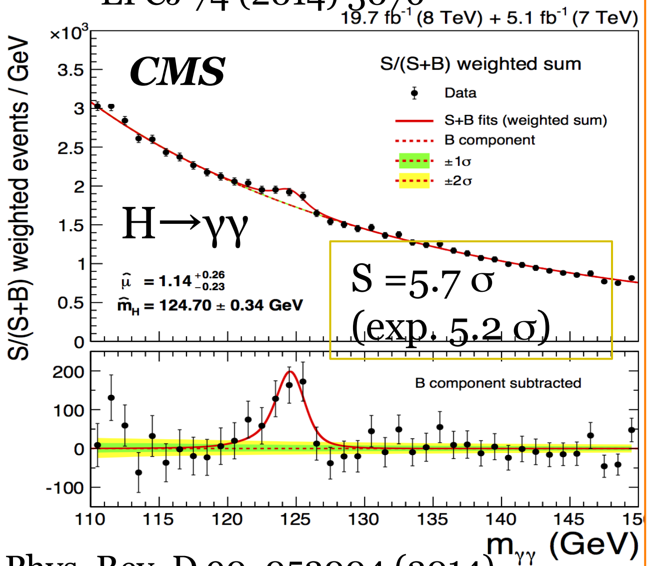

Phys. Rev. D 89 (2014) 092007

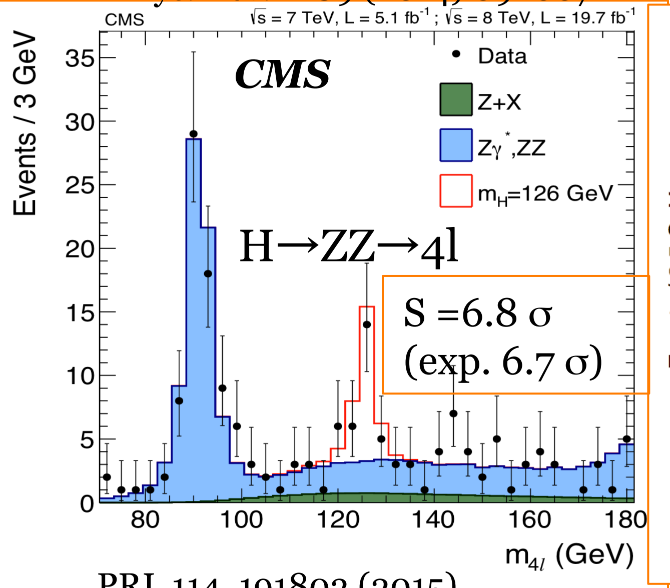

Phys. Rev. D 91, 012006 (2015)

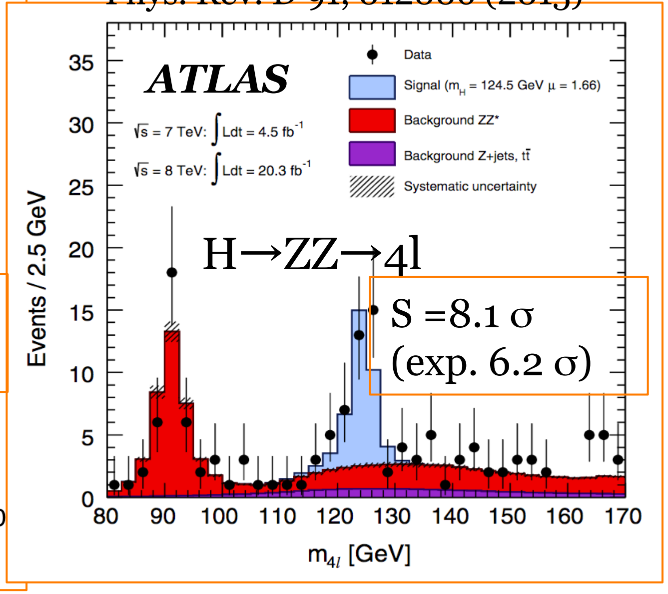

Phys. Rev. D 90, 052004 (2014)

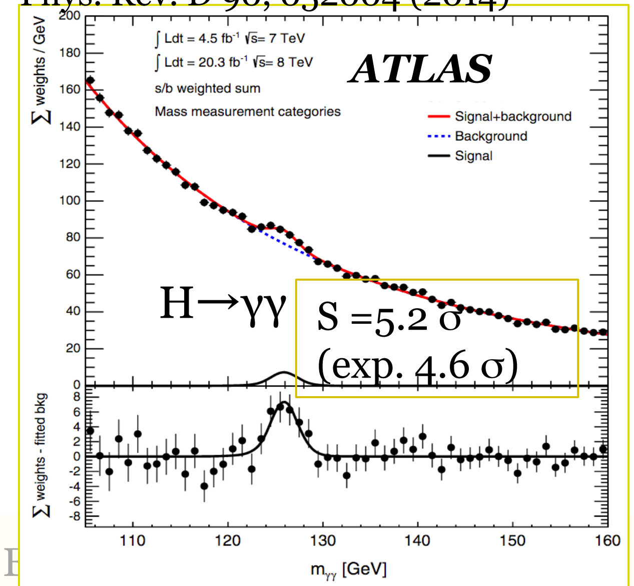

PRL 114, 191803 (2015)

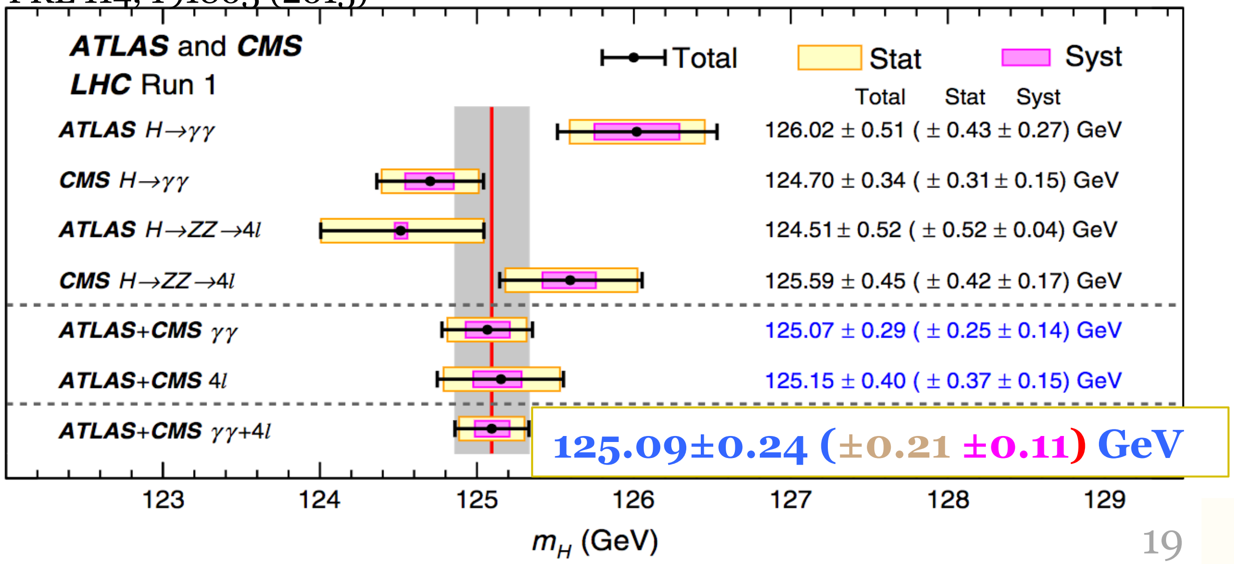

⑦ Higgs mass: H→γγ and H→ZZ→4l @ 13 TeV

HIG-16-020 (2nd Aug. 2016)

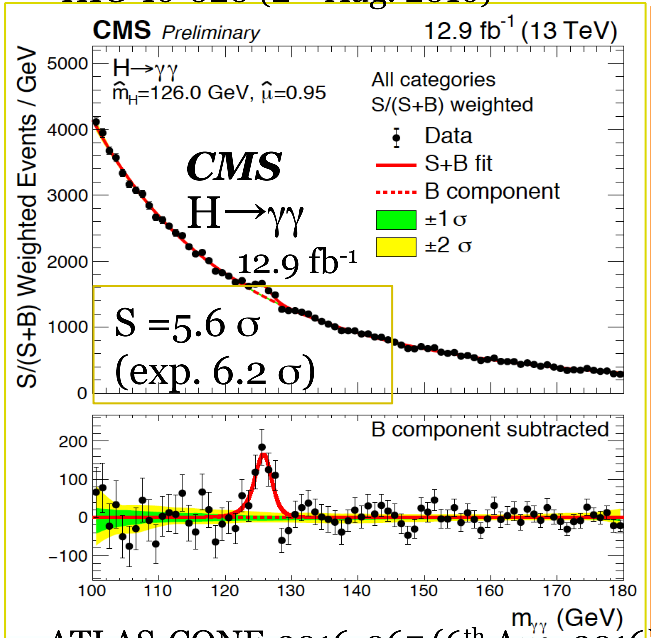

HIG-16-033 (2nd Aug. 2016)

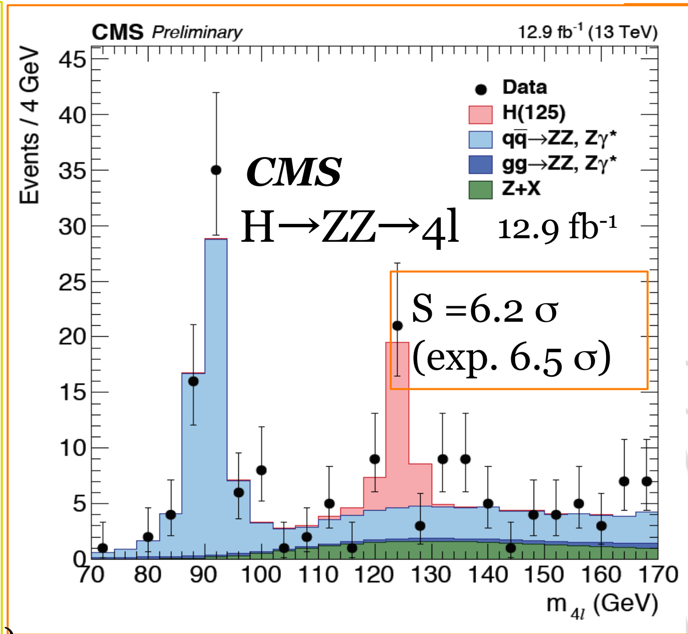

ATLAS-CONF-2016-079 (4th Aug. 2016)

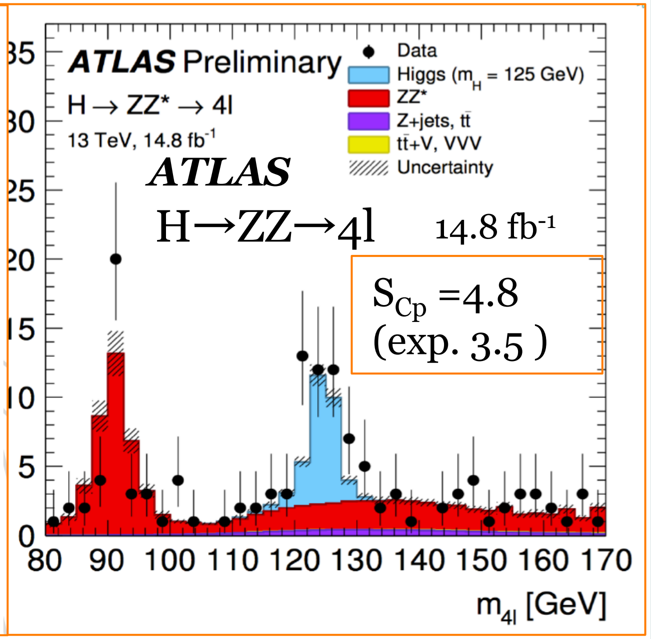

ATLAS-CONF-2016-067 (6th Aug. 2016)

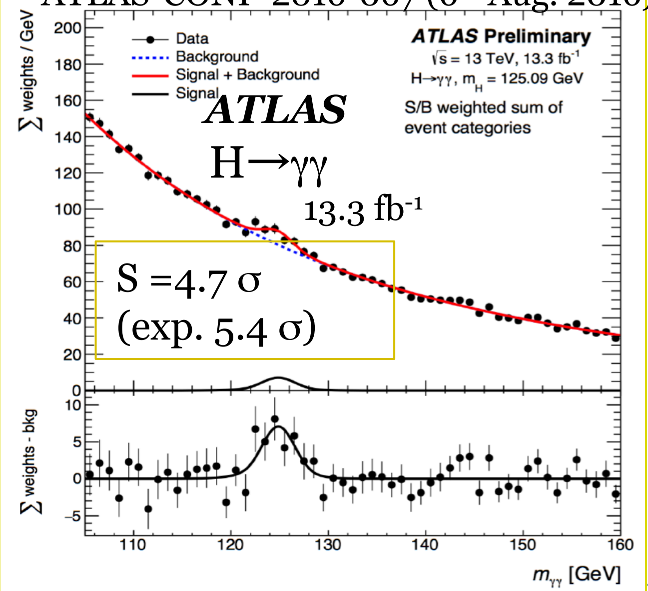

Significances at 125.09 GeV

Run 2 reached same sensitivity than Run 1

Search for an additional Higgs boson is performed for a range of masses up to 2.5 TeV and with various widths.

No significant excess has been observed.

(more in the “new physics searches” talk)

⑦ Higgs mass: H→γγ and H→ZZ→4l @ 13 TeV

SM 125 GeV Higgs

H→γγ

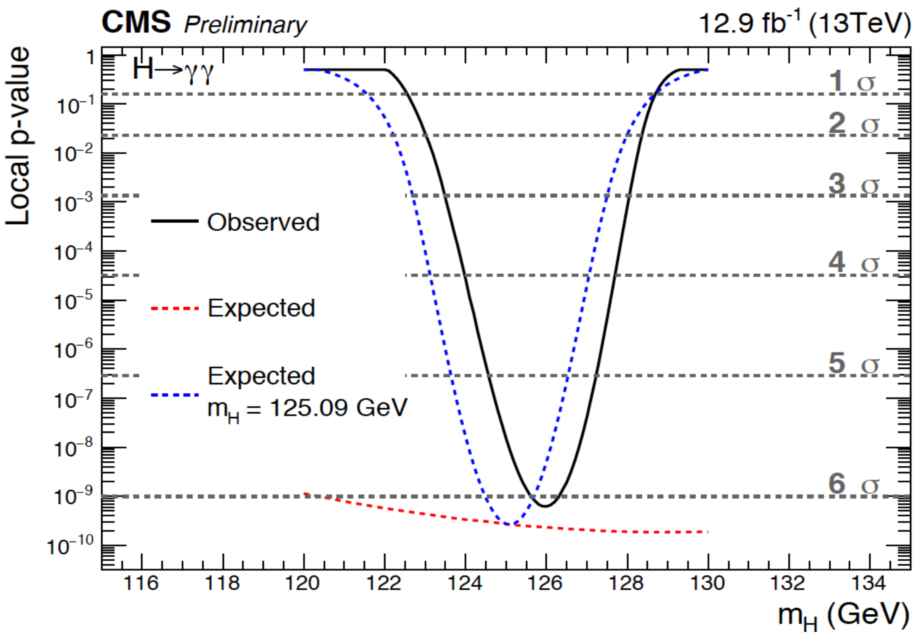

H→ZZ→4l

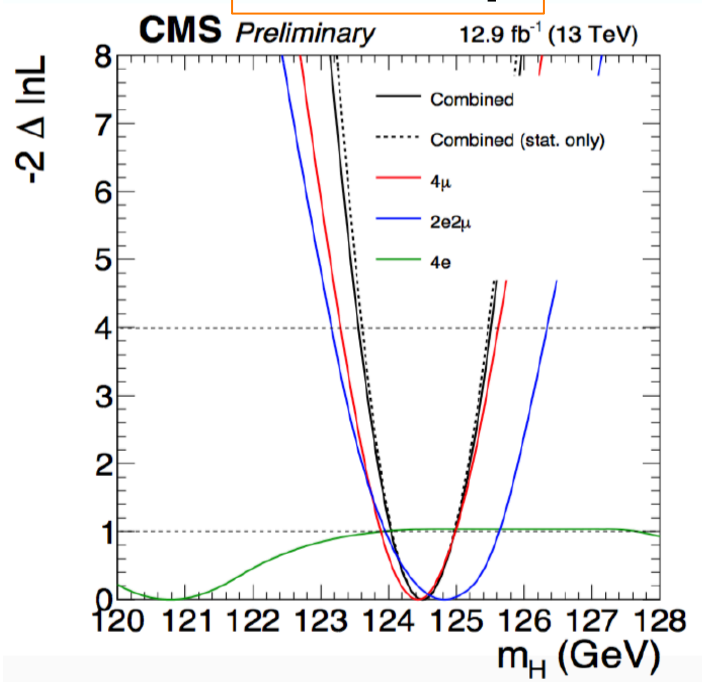

CMS γγ Run2: max. significance at 126.0 GeV

CMS γγ Run1: 124.70±0.34 GeV

CMS ZZ Run2: 124.50±0.48 GeV

CMS ZZ Run1: 125.59±0.45 GeV

ALTAS+CMS ZZ+γγ Run 1: 125.09±0.24 GeV

⑧ Higgs total cross section (√s)

ATLAS-CONF-2016-081

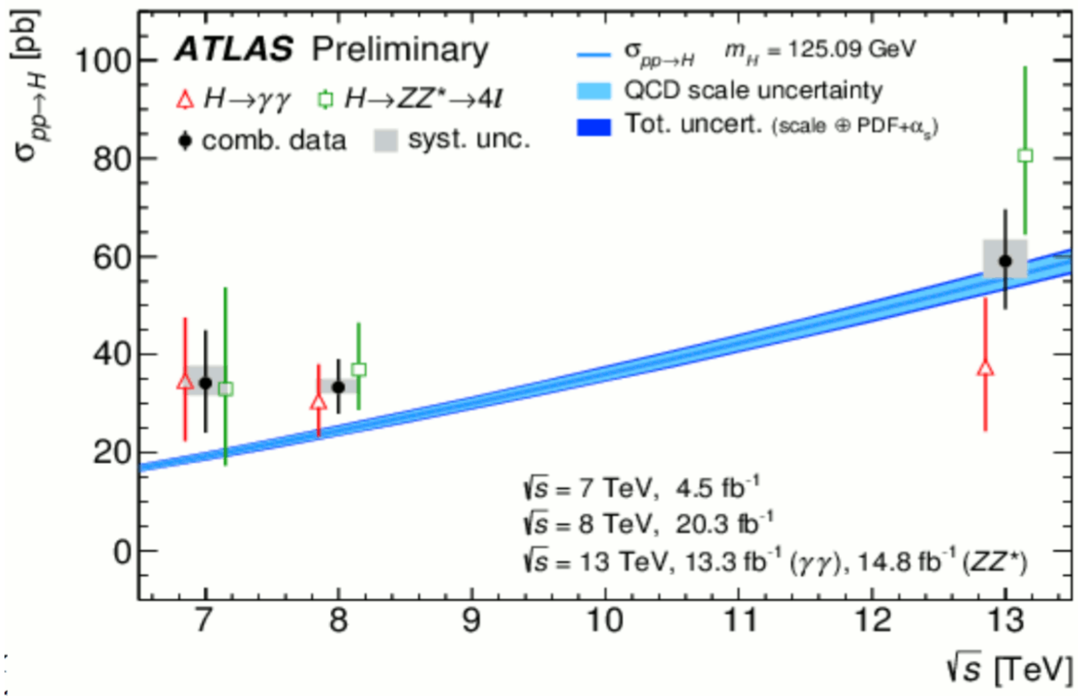

HIG-16-033

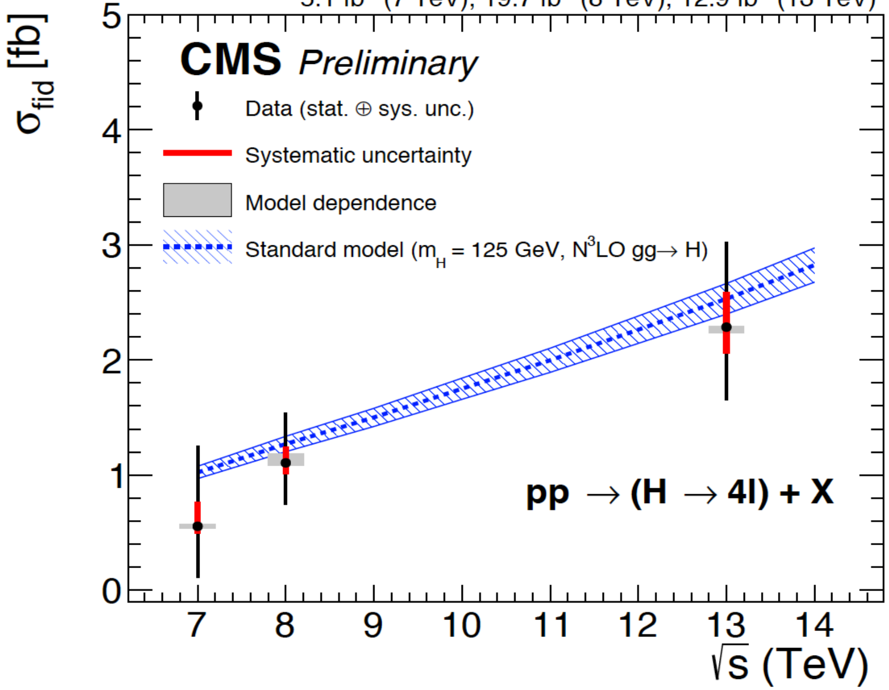

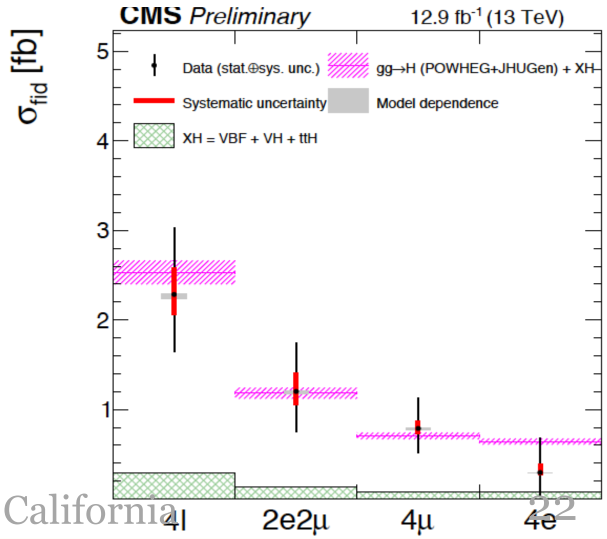

- ATLAS measured the Higgs total cross section
- CMS measured the cross section in the fiducial volume of the H→4l kinematic selection

Cross sections agree with SM within uncertainties

⑨ Higgs signal strength and coupling modifier

The signal strength, defined as the ratio of the measured Higgs boson rate to its SM prediction, is used to characterize the Higgs boson yields.
This ratio depends to the production cross section and to the brancing ratio:

production process "i"
decay channel "f"

$$\mu_i^f = \frac{\sigma_i}{(\sigma_i)_{SM}} \frac{BR_f}{(BR_f)_{SM}} = \frac{\sigma_i}{(\sigma_i)_{SM}} \frac{\Gamma_f / \Gamma_H}{(\Gamma_f / \Gamma_H)_{SM}}$$

For a given production process or decay mode, denoted "j", we define the coupling modifier:

$$k_j^2 = \frac{\sigma_j}{(\sigma_j)_{SM}}$$

or

$$k_j^2 = \frac{\Gamma_j}{(\Gamma_j)_{SM}}$$

$$\mu_i^f = k_i^2 k_f^2$$

If $\Gamma_H = (\Gamma_H)_{SM}$

some couplings are direct, others are "effective" due to loops.

production	coupling modifier
σ(ggF)	$1.06\, k^2_t + 0.01\, k^2_b + 0.01\, k_t k_b$
σ(VBF)	$0.74\, k^2_W + 0.26\, k^2_Z$
σ(WH)	k^2_W
σ(ttH)	k^2_t
σ(bbH)	k^2_b

decay	coupling modifier
Γ^{ZZ}	k^2_Z
Γ^{WW}	k^2_W
$\Gamma^{\gamma\gamma}$	$1.059\, k^2_W + 0.07\, k^2_t - 0.66\, k_t k_W$
$\Gamma^{\tau\tau}$	k^2_τ
Γ^{bb}	k^2_b

⑨ Higgs H→WW*, ττ, bb

H→WW*

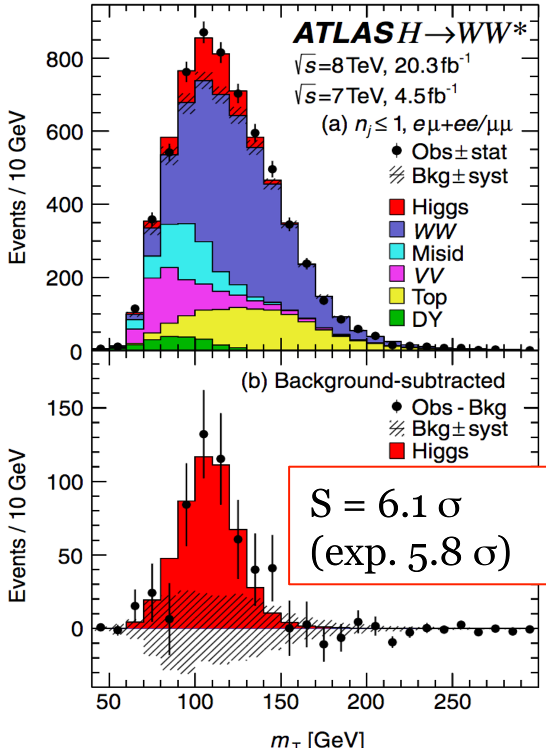

Phys. Rev. D 92, 012006 (2015)

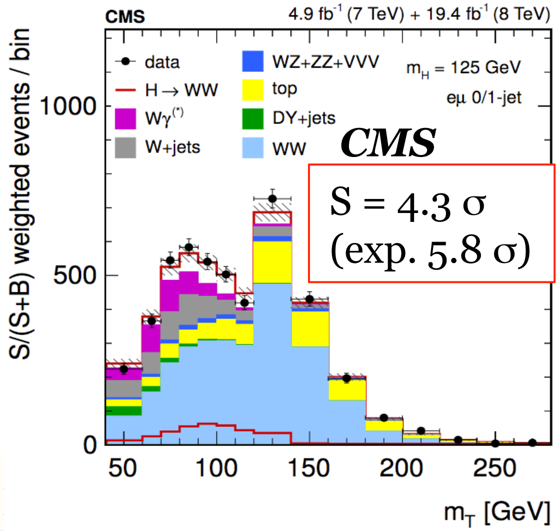

JHEP 01 (2014) 096

H→ττ

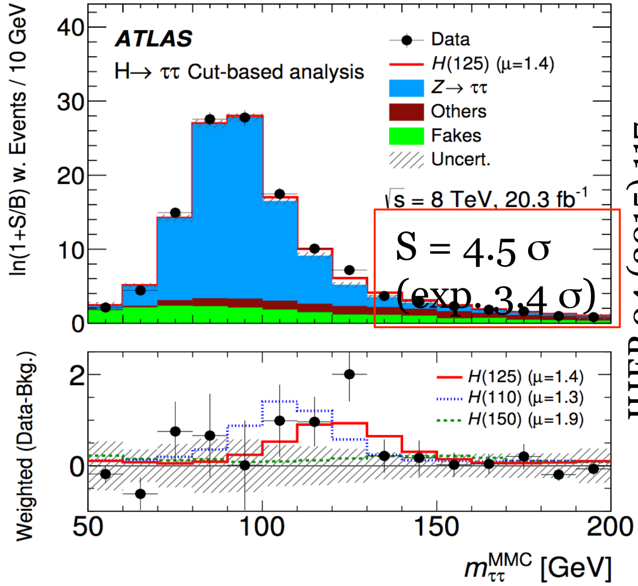

JHEP 04 (2015) 117

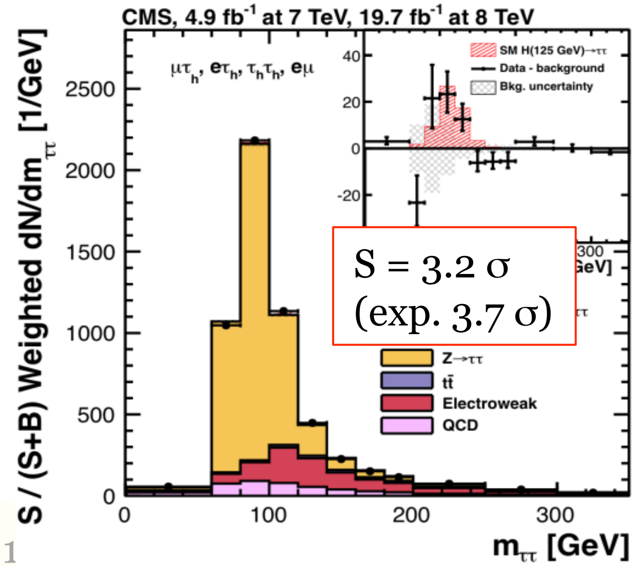

JHEP 05 (2014) 104

H→bb

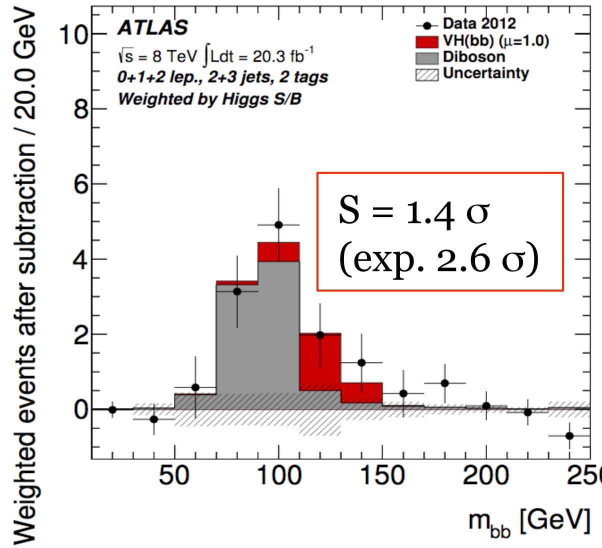

JHEP01(2015)069

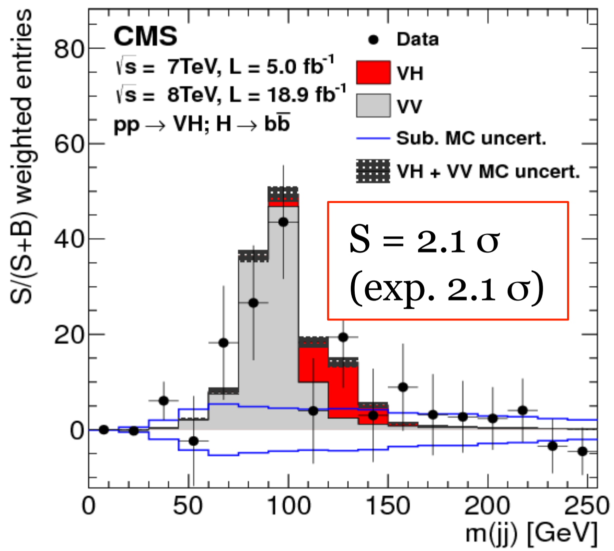

Phys. Rev. D 89 (2014) 012003

⑨ Higgs VBF, ttH, VH

VBF

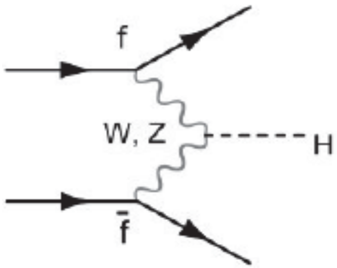

VH

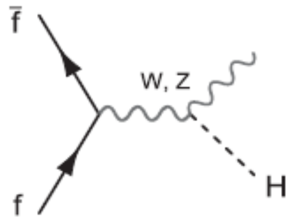

ttH

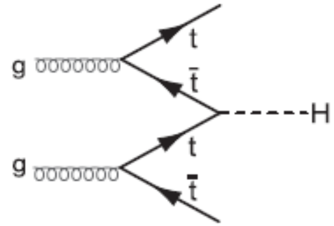

TAG

Two high pT jets with:

- high pseudorapidity separation
- form high invariant mass

Additional W or Z decay

Two additional bW

Channel categories	ATLAS/CMS			
	ggF	VBF	VH	ttH
γγ	✓	✓	✓	✓
ZZ (llll)	✓	✓	✓	✓
WW (lνlν)	✓	✓	✓	✓
ττ	✓	✓	✓	✓
H (bb)		✓	✓	✓

Run 1

Run 2

Tighter selection due to the tag
it allows softer selection in the decay:

No tag

$H \rightarrow ZZ \rightarrow 4l$

VH, ttH tag

$H \rightarrow ZZ \rightarrow 2l\ 2X$
$(X = l, \nu, q)$

⑨ Higgs signal strength and coupling modifier

Signal strength

arXiv:1606.02266 (7 June 2016)

σ•BR fit normalized to SM predictions.

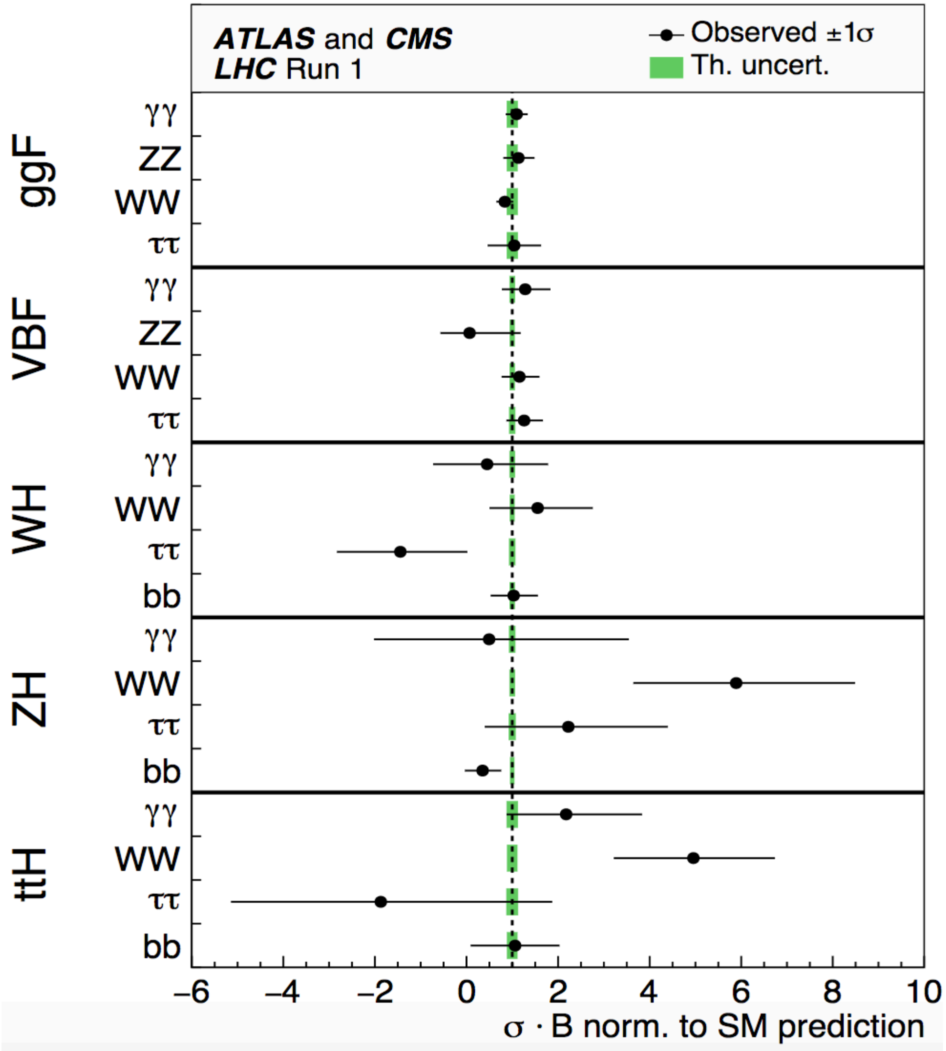

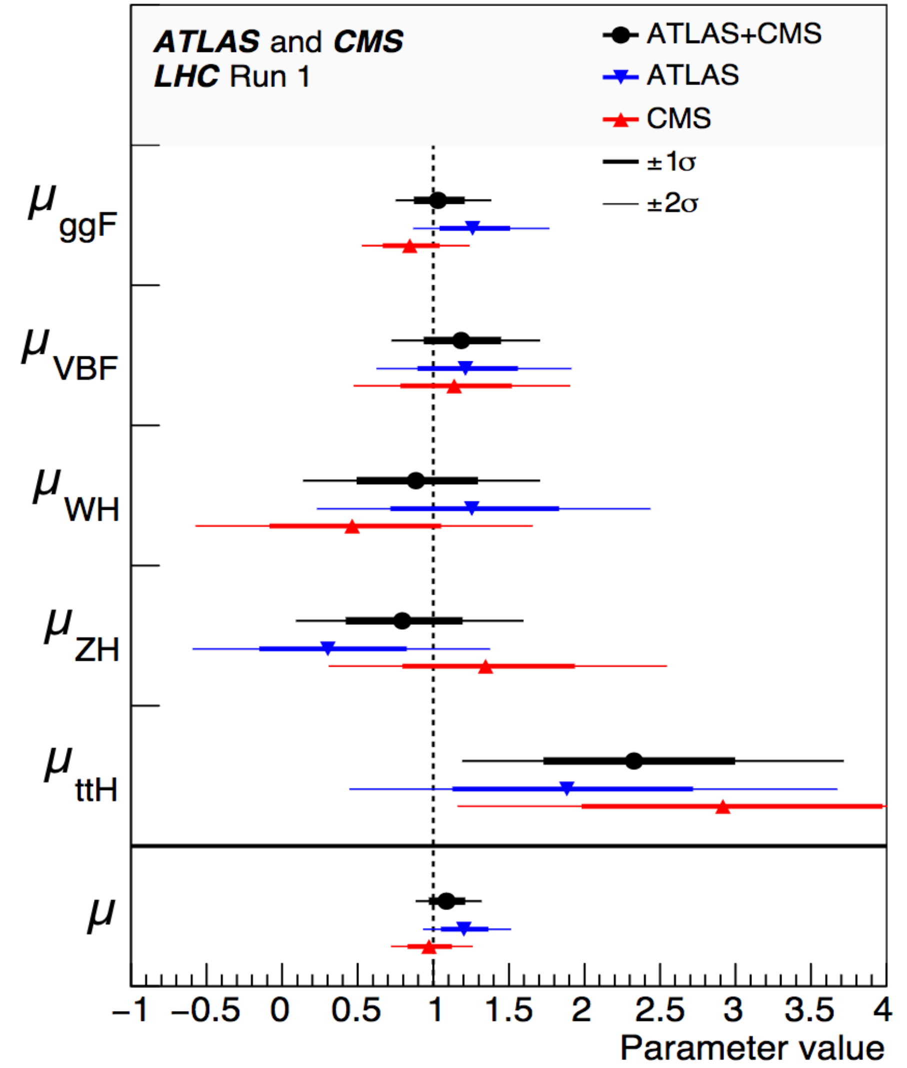

⑨ Higgs signal strength and coupling modifier

Coupling modifiers

best fit free $BR_{BSM} \geq 0$ best fit $BR_{BSM} = 0$

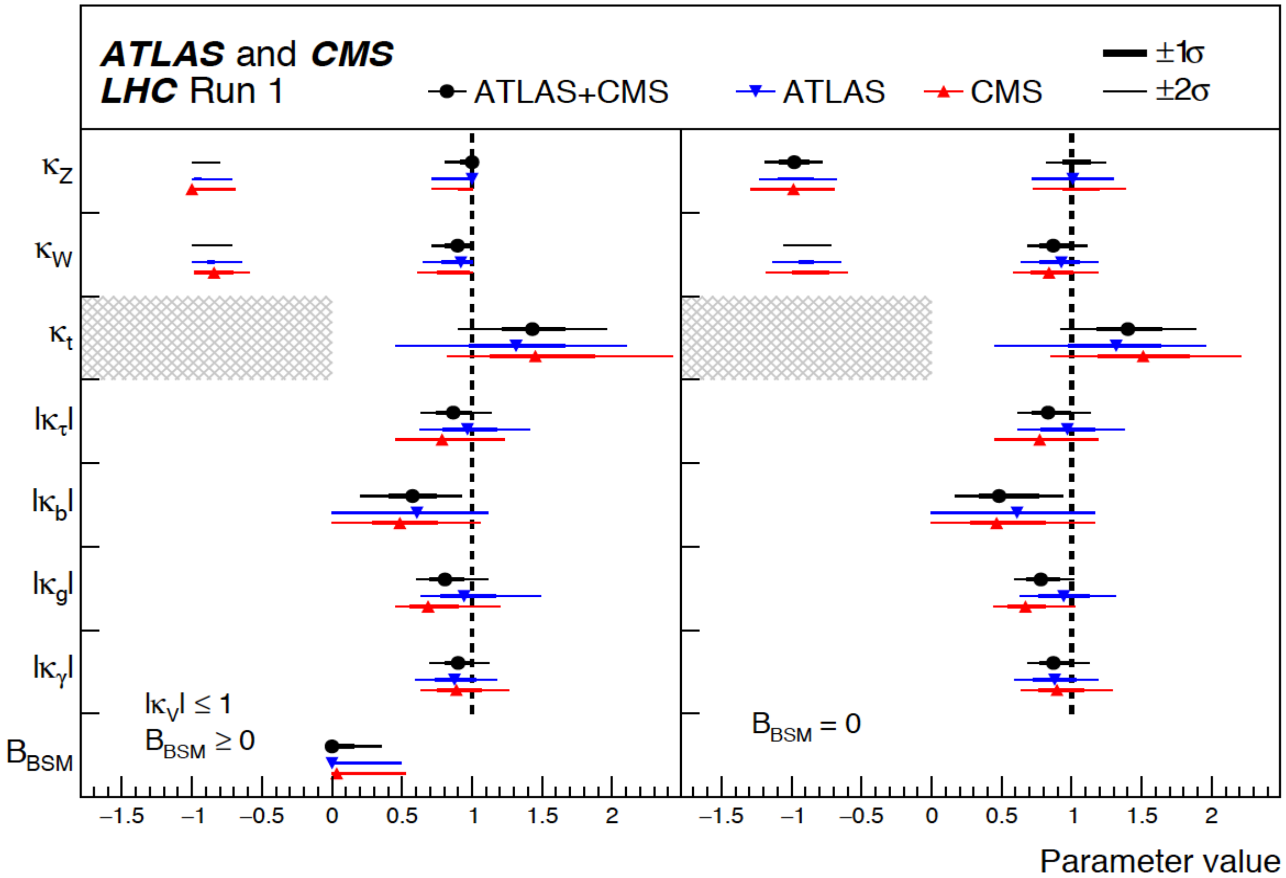

best fit k_g=1 and k_γ=1

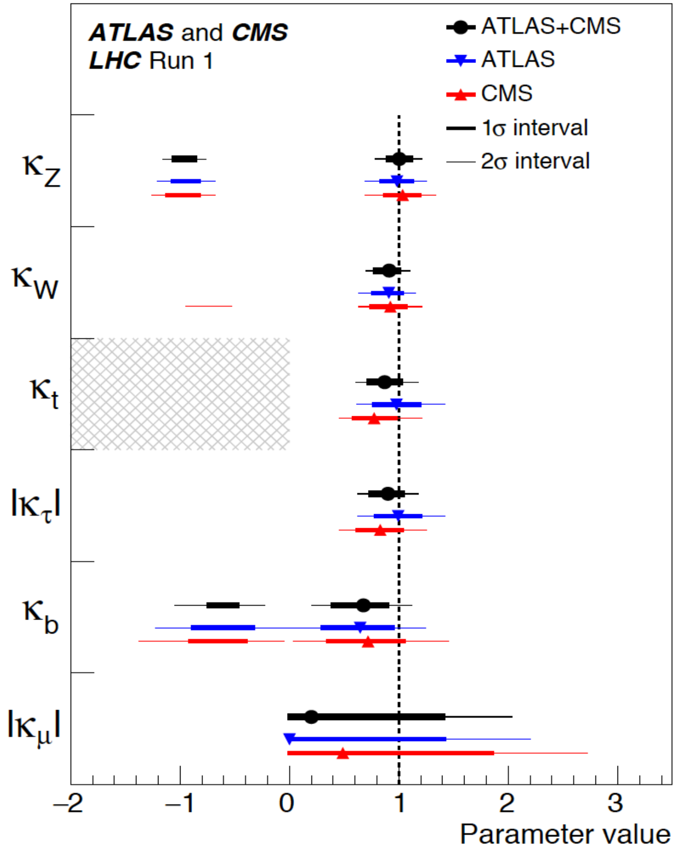

⑨ Higgs signal strength @ 13 TeV

H→ZZ→4l and H→γγ

ATLAS-CONF-2016-081

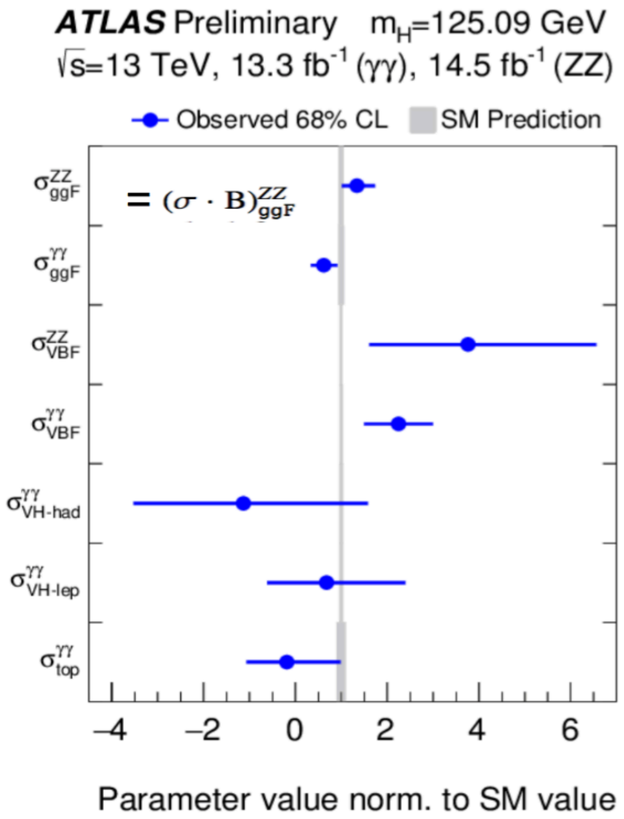

HIG-16-033

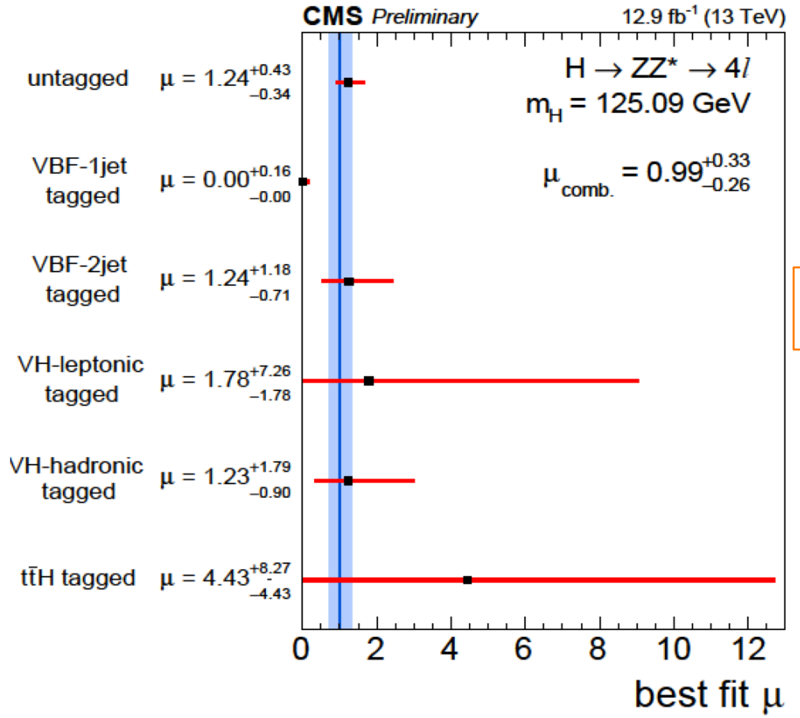

H→ZZ→4l

HIG-16-020

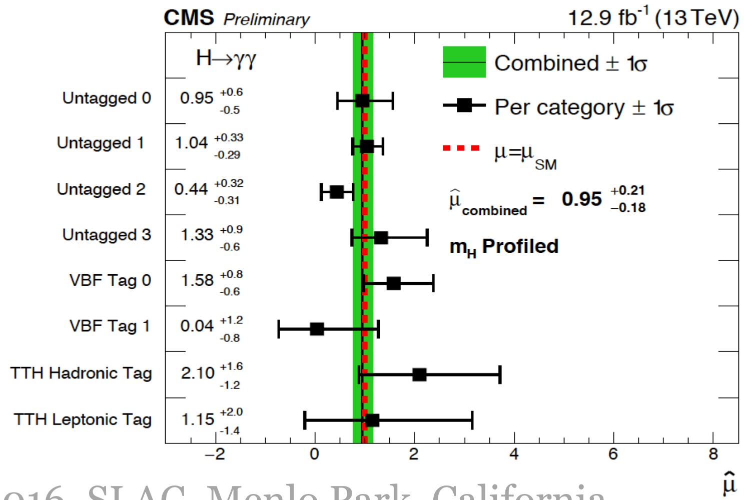

H→γγ

⑨ Small excess: ttH

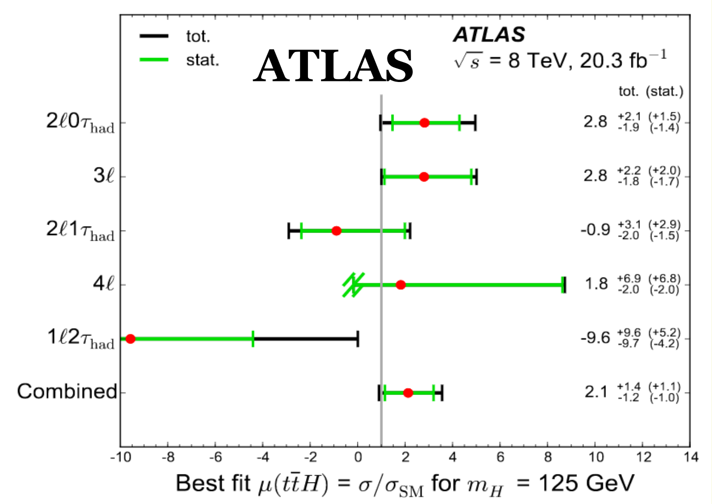

PLB 749 (2015) 519-541

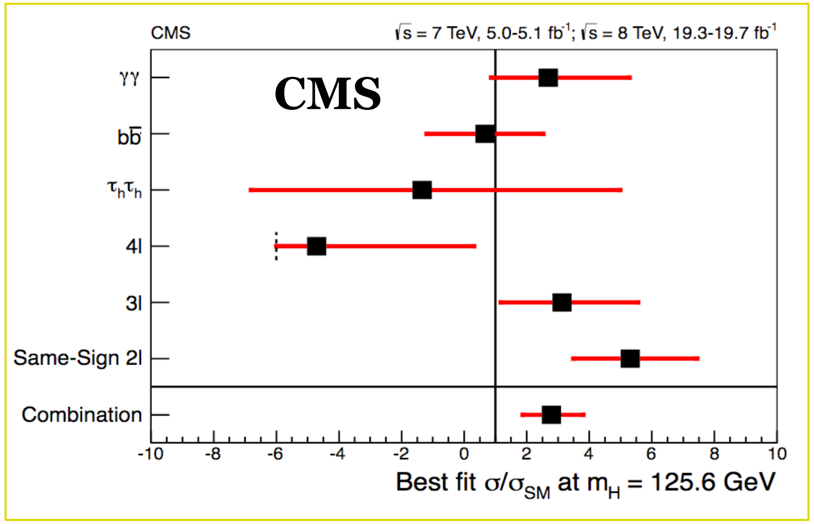

HEP 09 (2014) 087

Run 1

μ_{ttH} = 2.0±1.2 8 TeV

μ_{ttH} = 2.8±1.0 Run1

μ_{ttH} = 1.8±0.7 Run2

μ_{ttH} = 2.0±0.8 Run2 lept.

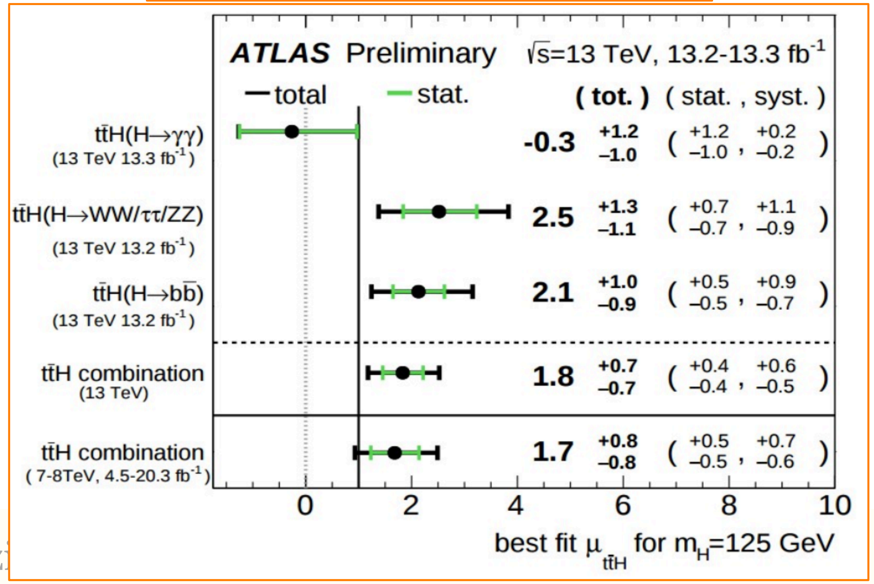

ATLAS-CONF-2016-068

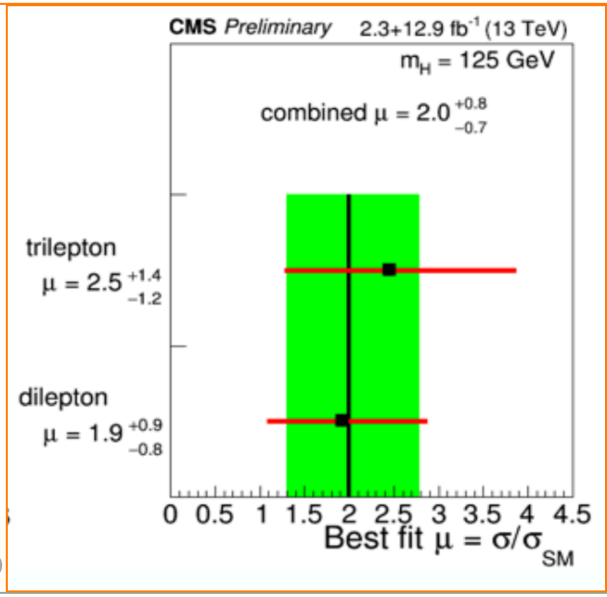

CMS PAS HIG-16-022

Run 2

⑩ Higgs decay width

Direct measurement of the Higgs boson width is not possible at a hadron collider unless $\Gamma_H > O(1)$ GeV or ~250 times larger than its Standard Model value (4.08 MeV @ 125.09 GeV). The cross section in the off-shell region can be used to extrapolate a limit for Γ_H/Γ_H^{SM} :

$$\frac{\sigma^{gg\to H^*\to ZZ}_{on-shell}}{\sigma^{gg\to H^*\to ZZ}_{on-shell,SM}} \approx \frac{k^2_{g,on-shell}\cdot k^2_{V,on-shell}}{\Gamma_H/\Gamma_H^{SM}} \qquad \frac{\sigma^{gg\to H^*\to ZZ}_{off-shell}}{\sigma^{gg\to H^*\to ZZ}_{off-shell,SM}} \approx k^2_{g,off-shell}\cdot k^2_{V,off-shell}$$

with the assumption that the coupling modifiers are the same in the on-shell and off-shell regions : $k_j^{on\text{-}shell} = k_j^{off\text{-}shell}$

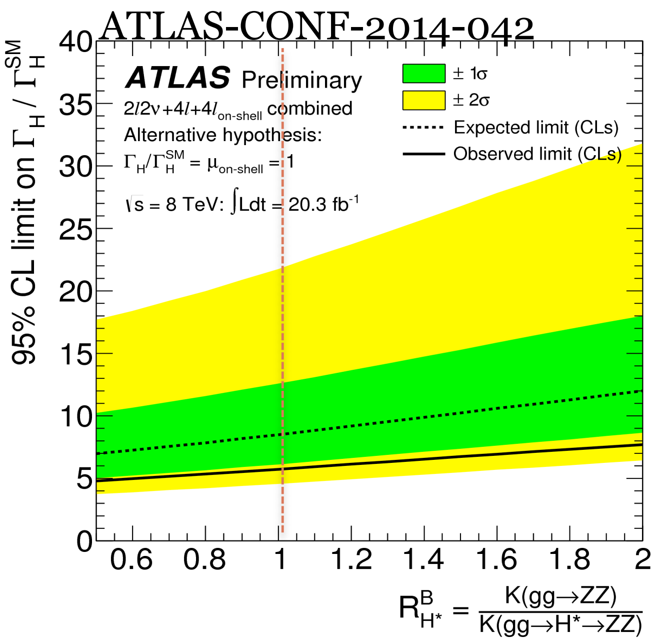

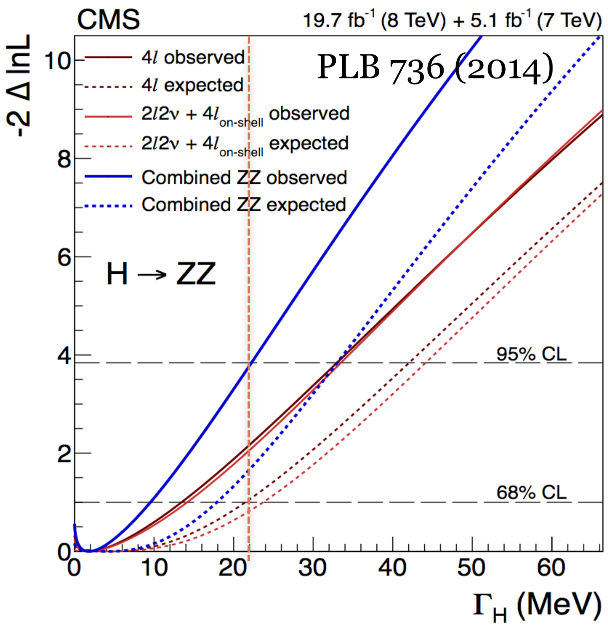

ATLAS

$\Gamma_H / \Gamma_H^{SM} < 5.7$ (95% C.L.)

(Off-shell: 220 GeV<m_{4l}<1000 GeV)
(M_H=125.5 GeV Γ_H^{SM}=4.14 MeV)

CMS

$\Gamma_H / \Gamma_H^{SM} < 5.4$ (95% C.L) ($\Gamma_H < 22 MeV$)

(Off-shell: 180 GeV< m_{4l})
(M_H=125.6 GeV Γ_H^{SM}=4.15 MeV)

11 Higgs spin and parity

The higgs spin and parity can be studied in the H→ZZ , H→WW and H→γγ channels
The SM Higgs boson hypothesis, corresponding to the quantum numbers $J^P=0^+$, is tested against several alternative spin and parity models.

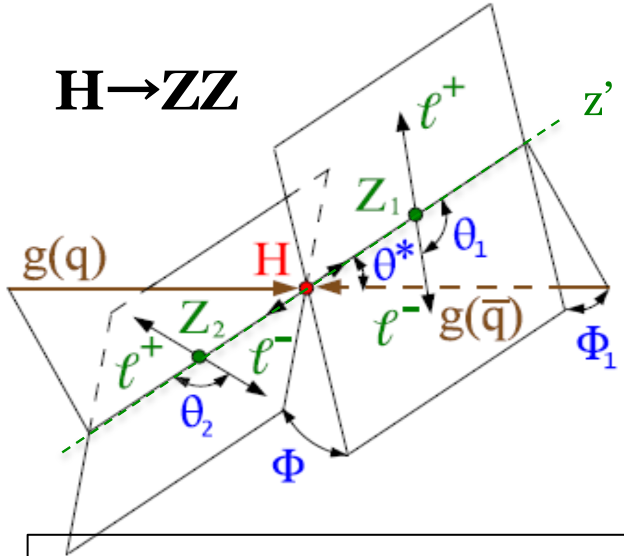

$$\vec{\Omega} = \{\theta^*, \Phi_1, \theta_1, \theta_2, \Phi\}$$

θ^* : angle between z' (Z_1Z_2 boson direction) and z axis

θ_1,θ_2: angles between the leptons and z'

Φ: angle between the two leptons pair planes

Φ_1 angle between z'z plane and two lept. plane

Discriminants

$$D_{J^P} = \frac{P_{SM}}{P_{SM}+P_{J^P}} = \left[1+\frac{P_{J^P}(m_{Z_1},m_{Z_2},\vec{\Omega}\,|\,m_{4l})}{P_{SM}(m_{Z_1},m_{Z_2},\vec{\Omega}\,|\,m_{4l})}\right]^{-1}$$

$$D_{bkg} = \frac{P_{sig}}{P_{sig}+P_{bkg}} = \left[1+\frac{P_{bkg}(m_{Z_1},m_{Z_2},\vec{\Omega}\,|\,m_{4l})\times P_{bkg}(m_{4l})}{P_{sig}(m_{Z_1},m_{Z_2},\vec{\Omega}\,|\,m_{4l})\times P_{sig}(m_{4l})}\right]^{-1}$$

Test statistic

The test statistic is defined using the ratio of signal plus background likelihoods for two signal hypotheses: **$-2\ln(\mathcal{L}_{JP} / \mathcal{L}_{0+})$**. The distribution of this ration is obtained by varying the nuissance parameters with gaussian distribution.

11 Higgs spin and parity

Eur. Phys. J. C75 (2015)

$J_P = 0^-$

Phys. Rev. D 89, 092007

$J_P = 1^+$

Phys. Rev. D 92, 012004

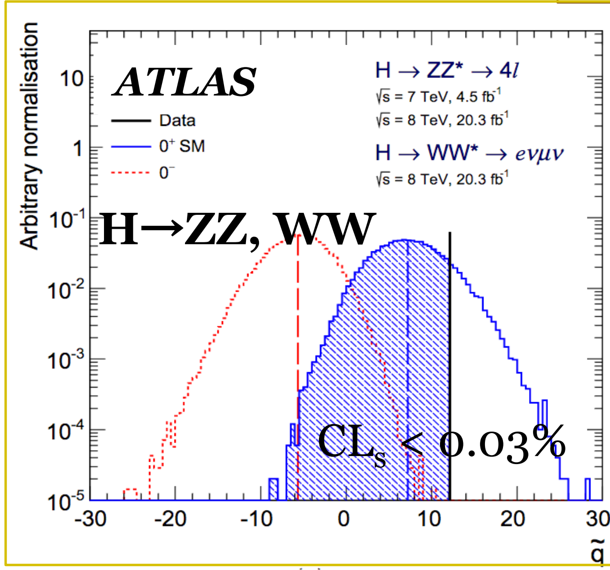

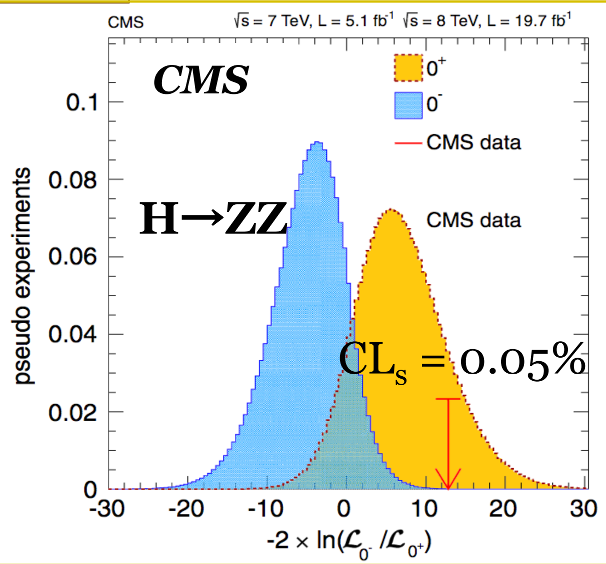

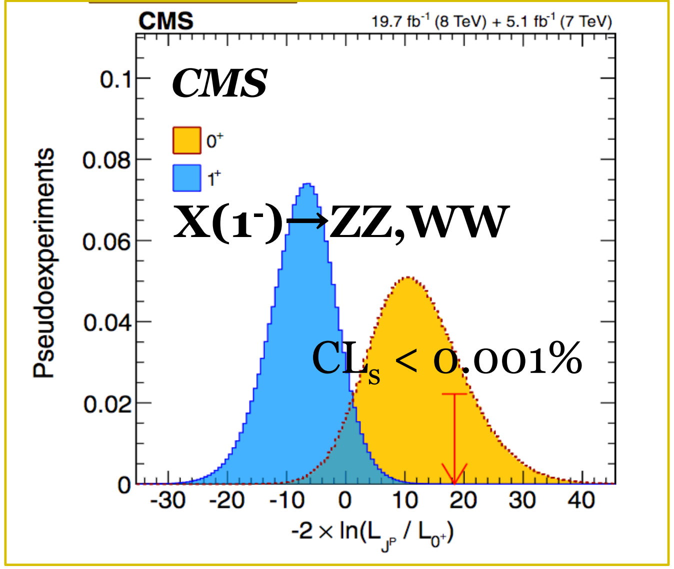

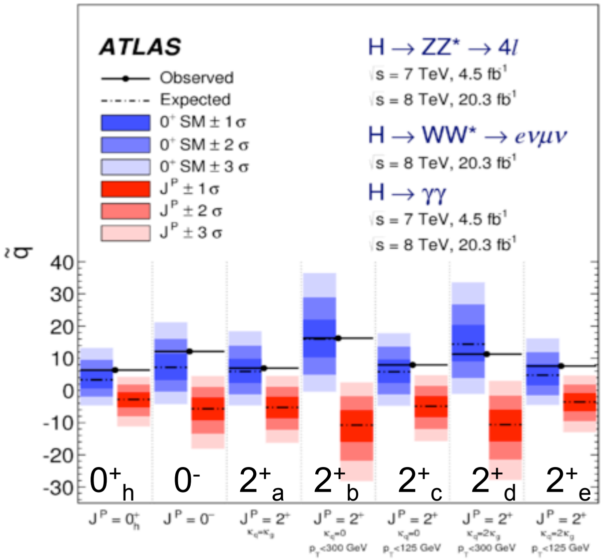

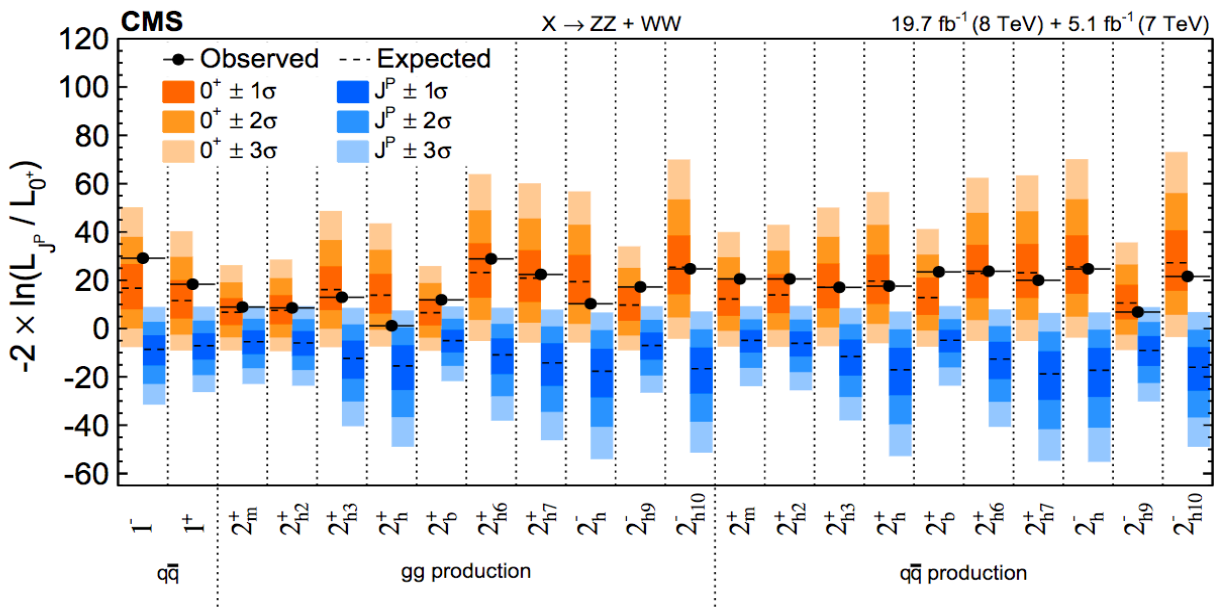

12 Outlook

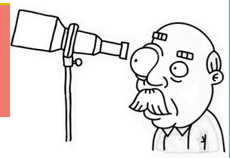

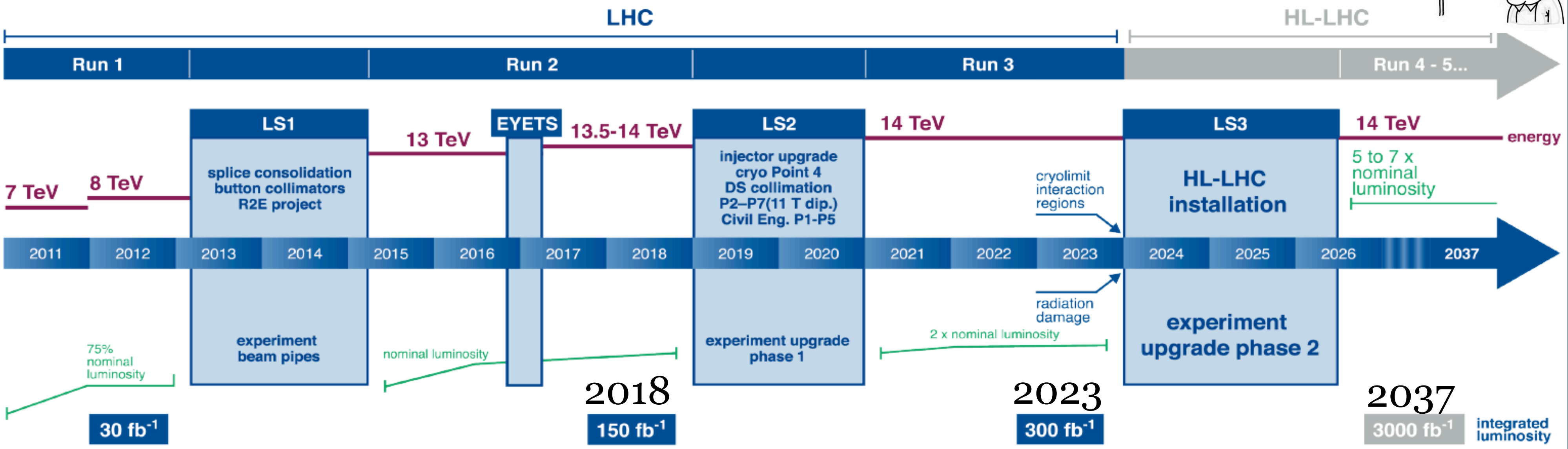

CERN-LHCC-2015-10

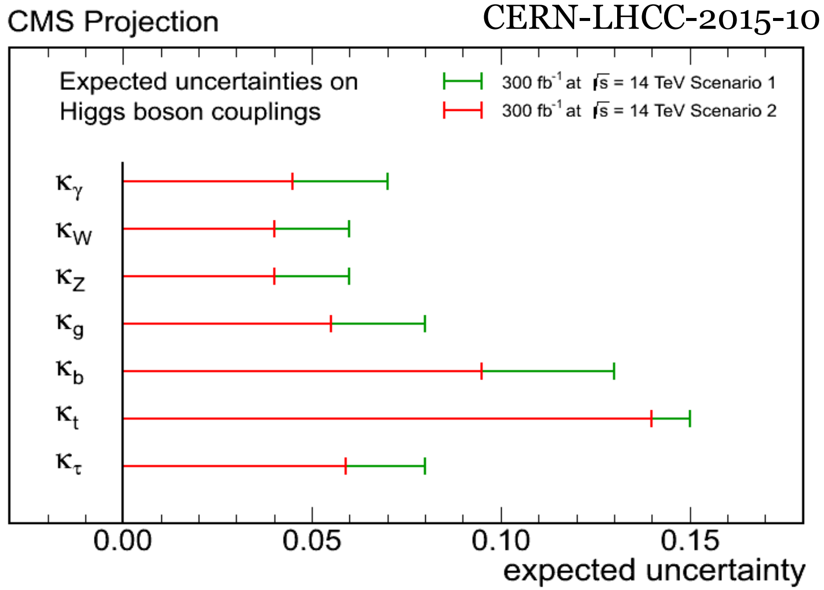

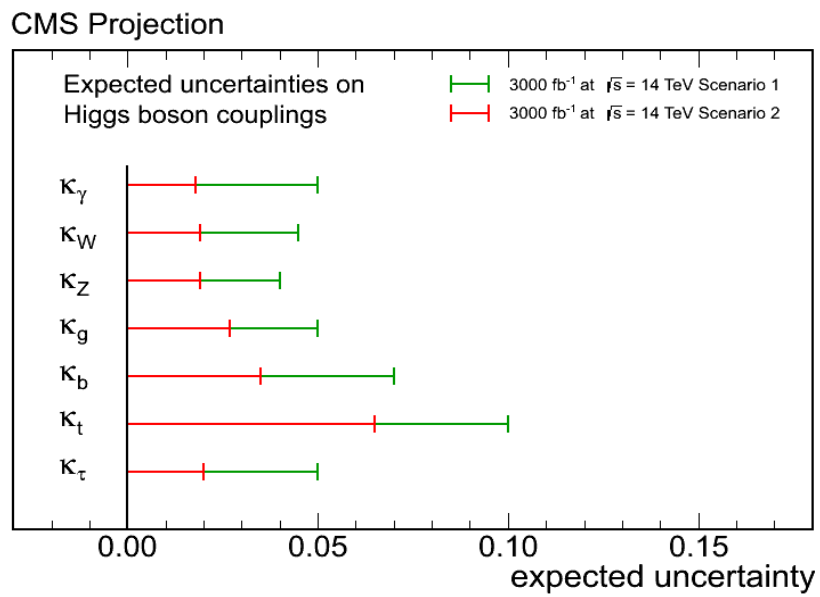

13 Summary

LHC run 1

- ✓ Cross sections for bosons and di-bosons are compatible with SM expectations, limits for the anomalous gauge couplings have been estimated.
- ✓ Top mass measured with a better precision than last Tevatron combination.
- ✓ Angular analysis of $B^0 \rightarrow K^* \mu^+ \mu^-$ (dB/dq^2, F_L, A_{FB}) compatible with SM, P'5 measurement expected soon.
- ✓ Several other SM tests not described here have been performed.
- ✓ Higgs boson has been discovered and his properties have been measured (mass, cross section, coupling parameters, decay with limit, spin and parity).
- ✓ Higgs boson looks SM like.
- ✓ Only few small excesses have been observed.

LHC run 2

- ✓ About 16 fb^{-1} have been analyzed, we expect 30 fb^{-1} for the end of the year.
- ✓ Run 2 and beyond:
  will provide more precise SM measurements;
  will characterize better the Higgs boson.
- ✓ No significant excess has been observed but there is still room for new physics.

Backup: Higgs decay width @ 13 TeV

HIG-16-033 (2 Aug. 2016)

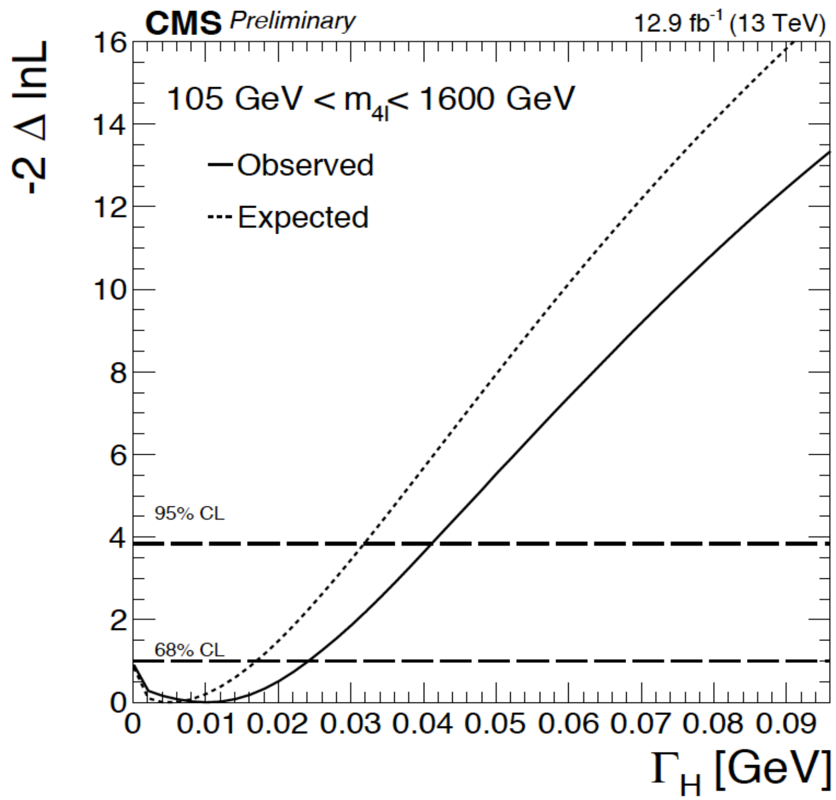

CMS

$\Gamma_H / \Gamma_H^{SM} < 9.9$ (95% C.L) $(\Gamma_H < 41\ MeV)$

Backup: X → γγ 13 TeV 16.2 fb^{-1}

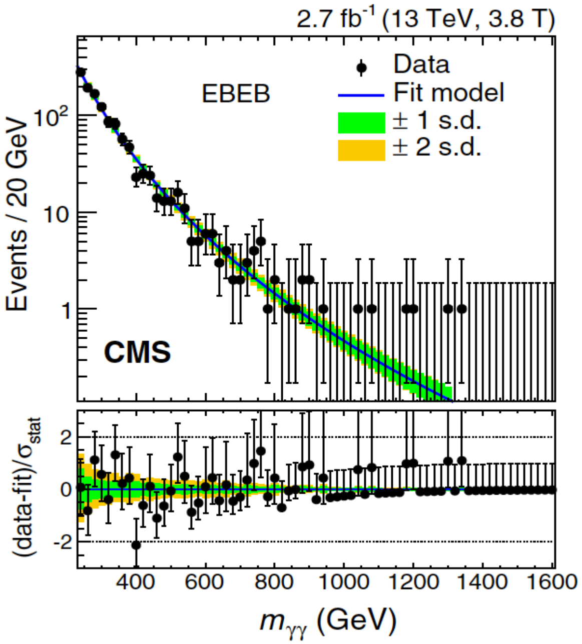

Phys.Rev.Let. 117(2016), no. 5, 051802

8 TeV (19.7 fb^{-1}) + 13 TeV (3.3 fb^{-1})

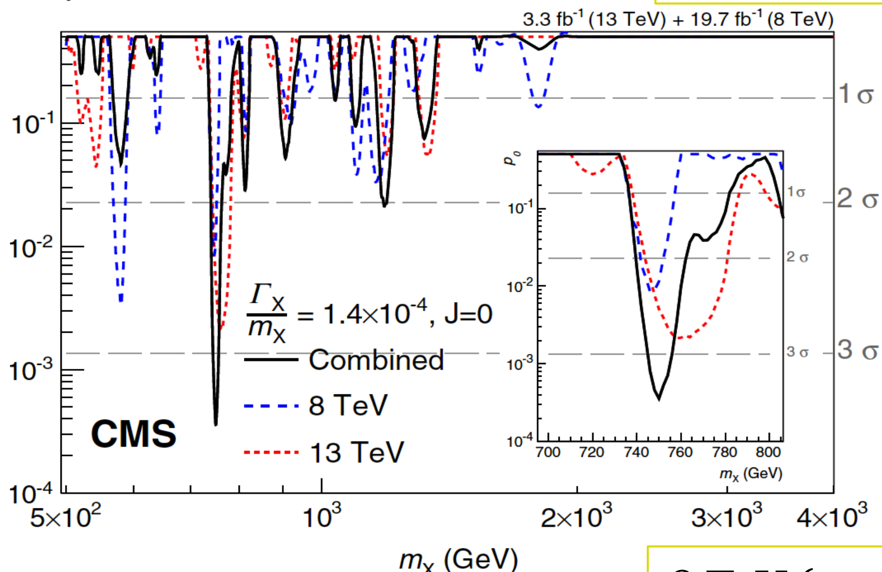

Largest excess observed for m_X = 750 GeV and narrow width hypotheses Γ_X/m_X=1.4 10^{-4}

Local significance:

3.4 σ

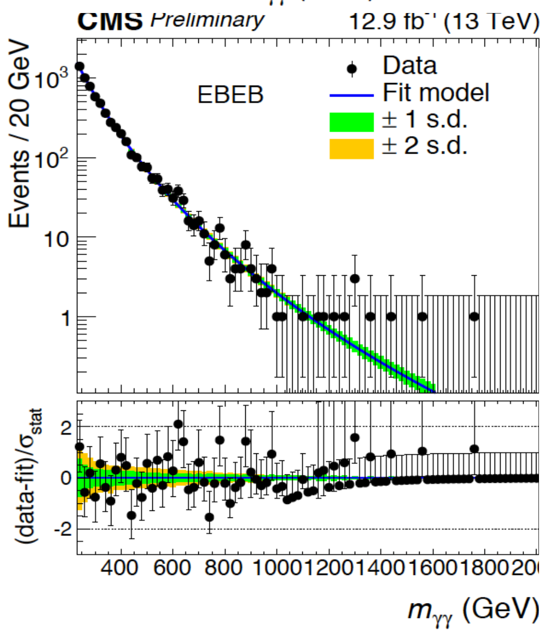

EXO-16-027

8 TeV (19.7 fb^{-1}) + 13 TeV (16.2 fb^{-1})

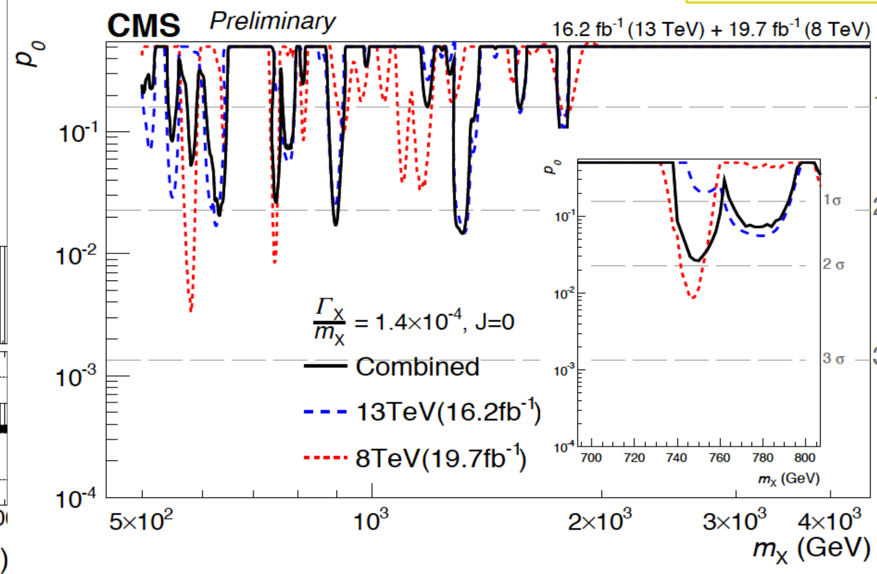

for m_X = 750 GeV and narrow width hypotheses Γ_X/m_X=1.4 10^{-4}

2015+2016

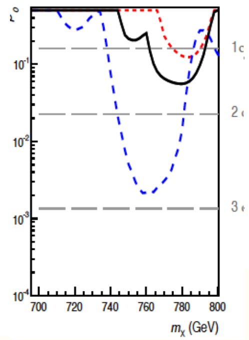

Local Significance:

1.9 σ

Backup: heavy Higgs search @ 13 TeV